https://doi.org/10.5194/acp-2020-1219
Preprint. Discussion started: 10 December 2020

Atmospheric Chemistry and Physics Discussions

Modelling the Impacts of Iodine Chemistry on the Northern Indian Ocean Marine Boundary Layer

Anoop S. Mahajan[1*], Qinyi Li[2], Swaleha Inamdar[1,3], Kirpa Ram[3], Alba Badia[4] and Alfonso Saiz-Lopez[2]

[1]Indian Institute of Tropical Meteorology, Ministry of Earth Sciences, Pune, 411016, India

[2]Department of Atmospheric Chemistry and Climate, Institute of Physical Chemistry Rocasolano, CSIC, Madrid, 28006, Spain

[3]Institute of Environment and Sustainable Development, Banaras Hindu University, Varanasi, 221 005, India

[4]Institute of Environmental Science and Technology (ICTA), Universitat Autònoma de Barcelona (UAB), Barcelona, Spain

* Corresponding author: Anoop S. Mahajan (anoop@tropmet.res.in); phone: +91 20 2590 4526

https://doi.org/10.5194/acp-2020-1219
Preprint. Discussion started: 10 December 2020

Atmospheric Chemistry and Physics Discussions

Abstract

Recent observations have shown the ubiquitous presence of iodine oxide (IO) in the Indian Ocean marine boundary layer (MBL). In this study, we use the Weather Research and Forecasting model coupled with Chemistry (WRF-Chem version 3.7.1), including halogens (Br, Cl and I) sources and chemistry, to quantify the impacts of the observed levels of iodine on the chemical composition of the MBL. The model results show that emissions of inorganic iodine species resulting from the deposition of ozone (O_3) on the sea surface are needed to reproduce the observed levels of IO, although the current parameterisations overestimate the atmospheric concentrations. After reducing the inorganic emissions by 40%, a reasonable match with cruise-based observations is found. A strong seasonal variation is also observed, with lower iodine concentrations predicted during the monsoon period when clean oceanic air advects towards the Indian subcontinent, and higher iodine concentrations predicted during the winter period, when polluted air from the Indian subcontinent increases the ozone concentrations in the remote MBL. The results show that significant changes are caused by the inclusion of iodine chemistry, with iodine catalysed reactions leading to regional changes of up to 25% in O_3, 50% in nitrogen oxides (NO and NO_2), 15% in hydroxyl radicals (OH), 25% in hydroperoxyl radicals (HO_2), and up to a 50% change in the nitrate radical (NO_3). Most of the large relative changes are observed in the open ocean MBL, although iodine chemistry also affects the chemical composition in the coastal environment and over the Indian subcontinent. These results show the importance of including iodine chemistry in modelling the atmosphere in this region.

Keywords: iodine, northern Indian Ocean, marine boundary layer, oxidising capacity

https://doi.org/10.5194/acp-2020-1219
Preprint. Discussion started: 10 December 2020

Atmospheric Chemistry and Physics Discussions

1. Introduction

Iodine compounds, emitted from the ocean surface, have been implicated in causing changes to the chemical composition of the marine boundary layer (MBL (Carpenter, 2003; Platt and Honninger, 2003; Saiz-Lopez et al., 2012a; Saiz-Lopez and von Glasow, 2012; Simpson et al., 2015). The known effects include changes to the oxidising capacity through the depletion of ozone (O_3) (Iglesias-Suarez et al., 2018; Mahajan et al., 2010b; Read et al., 2008; Saiz-Lopez et al., 2007) changes to the hydrogen oxides (HO_x = OH & HO_2) and nitrogen oxides (NO_x = NO and NO_2) concentrations (Bloss et al., 2005; Chameides and Davis, 1980) and oxidation of mercury (Wang et al., 2014). Coastal emissions of iodine compounds, through known biogenic sources such as macroalgae, have been shown to contribute significantly to new particle formation (McFiggans, 2005; O'Dowd et al., 2002, 2004). It has been suggested that even in the open ocean environments with low iodine emissions, it can participate in new particle formation (Allan et al., 2015; Baccarini et al., 2020; Sellegri et al., 2016). Recent ice-core observations in the high altitude Alps in Europe and in Greenland have shown an increase in the atmospheric loading of iodine compounds, which highlights the importance of understanding iodine cycling for accurate future projections (Cuevas et al., 2018; Legrand et al., 2018).

Over the last two decades, several field campaigns have focused on the measurement of iodine oxide (IO), which can be used as a proxy for iodine chemistry in the MBL. These observations made across the world show a near-ubiquitous presence of IO across the Pacific, Atlantic, and Southern Oceans with concentrations reaching as high as ~3 parts per trillion by volume (pptv) in the open ocean environment (Alicke et al., 1999; Allan et al., 2000; Commane et al., 2011; Furneaux et al., 2010; Gómez Martín et al., 2013; Großmann et al., 2013; Mahajan et al., 2012, 2009, 2010a, 2010b, 2011; Platt and Janssen, 1995; Prados-Roman et al., 2015; Read et al., 2008; Saiz-Lopez and Plane, 2004; Seitz et al., 2010; Stutz et al., 2007; Wada et al., 2007;

https://doi.org/10.5194/acp-2020-1219
Preprint. Discussion started: 10 December 2020

Atmospheric Chemistry and Physics Discussions

Zingler and Platt, 2005). Until recently, the Indian Ocean was the most under-sampled region for iodine species, but cruises that were a part of the Indian Southern Ocean Expeditions (ISOEs) and the International Indian Ocean Expedition- 2 (IIOE-2) have confirmed the presence of up to 1 pptv of IO in this region's MBL (Inamdar et al., 2020; Mahajan et al., 2019a, 2019b).

Over the Indian Ocean, intense anthropogenic pollution from Southeast Asia mixes with pristine oceanic air. The mixing of polluted continental and clean oceanic air masses results in unique chemical regimes, which change drastically due to distinct seasonal circulation patterns, such as the seasonally varying monsoon. During the winter monsoon season (November to March), high pollution levels are regularly observed over the entire northern Indian Ocean (Lelieveld et al., 2001), while during the summer monsoon (June-September), clean air dominates the atmospheric composition, leading to distinct chemical regimes (Lawrence and Lelieveld, 2010). For the other transitional months, especially the pre-summer monsoon period (March-June), the offshore pollution is in general weaker compared to the winter monsoon conditions (Sahu et al., 2006). The changing atmospheric composition over the Indian Ocean can interact with oceanic biogeochemical cycles and impact marine ecosystems, resulting in potential feedbacks. This is indeed the case of inorganic iodine emissions (hypoiodous acid, HOI and molecular iodine, I_2), which are considered to be the major sources of reactive iodine species from the ocean surface (Carpenter et al., 2013; MacDonald et al., 2014). The emission of both species depends on the deposition of atmospheric O_3, which shows a strong seasonal cycle due to the changes in the composition of the overlying airmasses. However, even though the emission of iodine compounds is expected to increase during higher pollution periods, anthropogenic NO_x can lead to titration of iodine in the atmosphere, leading to the formation of the relatively stable iodine nitrate ($IONO_2$), which effectively reduces the impact of iodine

https://doi.org/10.5194/acp-2020-1219
Preprint. Discussion started: 10 December 2020

Atmospheric Chemistry and Physics Discussions

on the atmosphere in terms of ozone depletion and also new particle formation (Mahajan et al., 2009, 2011, 2019b).

Recent modelling studies have made an attempt at quantifying the impact of iodine on a global scale (Saiz-Lopez et al., 2012b, 2014; Sherwen et al., 2016; Stone et al., 2018) and at regional scales (Li et al., 2019, 2020; Muñiz-Unamunzaga et al., 2018; Sarwar et al., 2015). Although both approaches have shown significant effects of iodine on the atmosphere, a strong difference is observed in different regions due to the existing chemical regimes. Amongst the regional studies, estimates in the eastern Pacific using the Weather Research and Forecasting model coupled with Chemistry (WRF-Chem) suggest that halogens account for about 34% of the total ozone depletion in the MBL, of which iodine compounds cause about 16% (Badia et al., 2019). In China, the contribution of iodine to the halogen-mediated effect on atmosphere oxidising capacity has been calculated to be up to 29% (Li et al., 2020). Using the Community Multiscale Air Quality Model (CMAQ), Li et al. (Li et al., 2019) showed that combined halogen chemistry (chlorine, bromine and iodine) induces variable effects on OH (ranging from -0.023 to 0.030 pptv) and HO_2 (in the range of -3.7 to 0.73 pptv), reduces nitrate radical (NO_3) concentrations (~20 pptv) and O_3 (by as much as 10 ppbv), decreases NO_2 in highly polluted regions (by up to 1.7 ppbv) and increases NO_2 (up to 0.20 ppbv) in other areas. Another study using the same model suggested that in the northern hemisphere, halogen chemistry, without higher iodine oxides photochemical breakdown, leads to a reduction of surface ozone by ~15%, whereas a simulation including their breakdown leads to reductions of ~48% (Sarwar et al., 2015).

However, studies are lacking in the quantification of the impact of iodine over the Indian Ocean MBL. Here, we study the effects of iodine chemistry on the atmospheric composition in the northern Indian Ocean MBL, a region where effects of iodine have not been studied hitherto, using the WRF-Chem model over three different periods in a year. We explore the geographical

https://doi.org/10.5194/acp-2020-1219
Preprint. Discussion started: 10 December 2020

Atmospheric Chemistry and Physics Discussions

and seasonal variability through quantification of iodine-mediated changes in ozone, HO_x and NO_x.

2. Methodology

The WRF-Chem model (version 3.7.1), which included a full halogen scheme (Cl, Br, and I) was used in the present study. The halogen chemistry scheme used in WRF-Chem and a detailed description of the model setup are described in past studies (Badia et al., 2019; Li et al., 2020). Sources of reactive iodine species considered in this study are an oceanic source of organic iodine compounds (CH_2ICl, CH_2IBr, CH_2I_2, and CH_3I) and inorganic compounds from the ocean surface (HOI and I_2). The sea-to-air fluxes of organic compounds were calculated online (Liss and Slater, 1974). The oceanic emission of inorganic iodine (HOI and I_2), which is dependent on the deposition of O_3 to the surface ocean and reaction with iodide (I^-) was calculated online using a parameterisation based on Badia et al. (2019), which was computed using the empirical laboratory measured parameterisations by Carpenter et al. (2013) and MacDonald et al. (2014). These emissions produced much higher than observed levels of IO in the northern Indian Ocean MBL. The reasons for the overestimation are discussed further in Section 3.2. Hence for the rest of the analysis, the emissions of I_2 and HOI were reduced by 40% (i.e. 60% of the standard emission parameterisation).

The domain for the simulations was selected to cover the Indian subcontinent and the northern Indian Ocean (as shown in Figure 1). We used a spatial resolution of 27 km and 30 vertical layers (sigma levels of 1.00, 0.99, 0.98, 0.97, 0.96,0.95, 0.94, 0.93, 0.92, 0.91,0.89, 0.85, 0.78, 0.70, 0.60,0.51, 0.43, 0.36, 0.31, 0.27,0.23, 0.20, 0.17, 0.14, 0.11,0.08, 0.05, 0.03, 0.02, 0.01, 0.00) with the surface layer ~20 m above ground level and 10 layers within the boundary layer. The simulation period included three seasons in the year of 2015 (pre-monsoon in April;

https://doi.org/10.5194/acp-2020-1219
Preprint. Discussion started: 10 December 2020

Atmospheric Chemistry and Physics Discussions

summer monsoon in July; and the winter monsoon period in January). We ran the WRF-Chem model for the months of January, April and July with an extra spin-up period of 15 days. The reason for choosing these three months is the different chemical regimes that result over the Indian Ocean due to changing meteorological conditions. Figure 1 shows the monthly averaged wind direction and speed over the northern Indian Ocean, which shows the drastic differences in air masses over the three seasons. Using these considerations, three sets of simulations were conducted. The BASE scenario considered no iodine emissions from the ocean surface; the orgI scenario considered only emissions of organoiodides as mentioned above; and the HAL scenario considered emissions of both inorganic iodine and the organoiodides. Changes in atmospheric compositions between BASE and HAL represent the impact of the overall iodine sources and chemistry; while those between the BASE and orgI scenarios represent the impact of organic iodine emissions; and the difference between orgI and HAL shows the impact of inorganic emissions of iodine from the ocean surface (HOI and I_2).

The model results were validated using observations from cruise-based campaigns in the Indian Ocean, i.e. during the 2nd International Indian Ocean Expedition (December 2015) and the 8th Indian Southern Ocean Expedition (ISOE-8) (January 2015) (Mahajan et al., 2019b, 2019a). Unfortunately, observations were available only during the winter monsoon period, and hence no direct validation was possible during the other seasons. Observations of IO in the MBL, along with surface ozone concentrations, were used for the validation of the model simulations. The MBL in the model results was defined as the lowest 10 layers (1.0 km above sea level). The domain chosen for the model simulations, along with the tracks of the cruises from which data was used for validation are shown in Figure 2.

3. Results and Discussions

https://doi.org/10.5194/acp-2020-1219
Preprint. Discussion started: 10 December 2020

Atmospheric Chemistry and Physics Discussions

3.1 Model validation

A comparison between the model simulated IO and O_3 from the HAL scenario and observations made during the IIOE-2 and 8th ISOE expeditions is shown in Figure 3. The top panel shows a comparison between the modelled and observed IO mixing ratios, with both the model and observations showing IO values below 1 pptv for all the locations. For most of the data points, the model simulated IO is slightly higher than the observations, although within the uncertainty. It should be remembered that this close match is after reducing the emissions of inorganic iodine species from the ocean surface by 40% (discussed further is Section 3.2). The largest mismatch is observed close to 5º N, where the model predicts approximately 0.9 pptv, while the observations show a low of 0.23±0.16 pptv. A point to note is that the IIOE-2 observations were from December 2015, and hence an exact match is not expected. Nonetheless, the comparison shows that the model does a good job at reproducing the levels of IO observed in the northern Indian Ocean. The levels observed and simulated IO are similar to the west Pacific (Badia et al., 2019) and in the South China sea (Li et al., 2020) but lower than the modelled and observed values of ~1.5 pptv in the tropical Atlantic MBL (Mahajan et al., 2010b).

The bottom panel of Figure 3 shows a comparison between the model simulated O_3 with the observations. Although the match between the model and observations is good in the northern Indian Ocean, there is a mismatch in the open ocean closer to the equator, with the model predicting higher values than the observations. The decreasing trend towards the open ocean is well captured by the model, with higher values observed close to the Indian coast where larger anthropogenic emissions are present. The average overestimation of ozone across all the locations where observations were available was ~25%. The model captures well the difference between the IIOE-2 and the ISOE-8 cruises, which started from the west and east coasts of India, respectively. Larger values of O_3 were observed during the ISOE-8, which were seen in

https://doi.org/10.5194/acp-2020-1219
Preprint. Discussion started: 10 December 2020

Atmospheric Chemistry and Physics Discussions

the model simulations too, and shows that the O_3 concentrations during the winter months are higher to the east of India as compared to the west.

3.2 Geographical distribution of IO

Figure 4 shows the geographical distribution of daytime averaged IO across the selected domain during the three seasons, for the orgI and HAL cases, along with the difference between the two. The orgI scenario shows significantly low values across the domain, with a peak of only 0.06 pptv (in January) in the western Indian Ocean close to the equator (Figure 4, top panels). When averaged across the whole domain for the boundary layer, the mean IO mixing ratio is a negligible 0.011±0.009 pptv in January, 0.008±0.006 pptv in April and 0.012±0.009 pptv in July (Table 1). Even if only the MBL is considered after applying a land mask, the mean IO mixing ratio is only 0.015±0.009 pptv in January, 0.011±0.006 pptv in April and 0.015±0.008 pptv in July (Table 1). At such low concentrations, iodine chemistry would not have any measurable impact on atmospheric chemistry. The values closer to the Indian subcontinent are negligible, although a high of ~0.04 pptv is seen close to the western Indian and Pakistani coast during the summer monsoon period (July). It is well known that this region experiences strong mixing in the northern Arabian sea during the summer monsoon period, which triggers plankton blooms resulting in high productivity (Qasim, 1982). For the current model runs, emissions of organic iodine are based on a climatology concentration of organic halogens in the sea water (Ziska et al., 2013), which show high organoiodides emissions in this region. However, despite the being an area of high productivity, the values of IO predicted in the orgI scenarios are significantly lower than the observations (by a factor of 10-20; Figure 2) and show the need for an inorganic iodine flux. Such a flux has been suggested to be ubiquitous and dependent on the ozone deposition and seawater iodide concentrations (Carpenter et al., 2013; MacDonald et al., 2014).

https://doi.org/10.5194/acp-2020-1219
Preprint. Discussion started: 10 December 2020

Atmospheric Chemistry and Physics Discussions

The middle panels in Figure 4 show the distribution of IO for the HAL scenario, which includes an inorganic iodine flux of I_2 and HOI as mentioned earlier. The flux strength has been reduced by 40% (i.e. 60% of the standard emission parameterisation) compared to the past studies to get a closer match between the observations and the model. Without such a reduction, the model predicts a peak of ~1.7 pptv in the domain, which is almost double the peak value observed during the IIOE-2 or ISOE-8, even when the uncertainty in the observations is considered (Figure 2). The main drivers for a sea-to-air flux of HOI and I_2 are the concentration of iodide in the seawater and the atmospheric ozone concentrations. The seawater iodide concentration in the model was estimated using the MacDonald et al. (2014) parameterisation, which is based on the sea surface temperature. This is also the largest uncertainty in the inorganic iodine emissions parameterisation. Recent studies have shown that the MacDonald et al. parameterisation underestimates the seawater iodide in the Indian Ocean (Inamdar et al., 2020), with the model predicted mean iodide in the domain being 117.4±1.4 nM (range: 113 to 119 nM). Ship-based observations in the same region show a mean iodide value of 185.8±66.0 nM (range of 100 to 320 nM) (Chance et al., 2019, 2020). Iodide observations were unfortunately not made during the same time as the model runs, but it is unlikely that the model overestimates the iodide considering the range of reported observations. Indeed, if we use the mean observed values for the seawater iodide concentrations, the I_2 flux would increase by ~58% and HOI flux would increase by 44%, rather than both decrease by 40% as necessary. The second reason for overestimating the sea-to-air iodine flux could be the overestimation of ozone in the model. The model overestimates the ozone by ~25% across all the locations where ozone observations were available (Figure 3). This would cause a ~20% larger flux of HOI and I_2 as compared to the observed O_3 values. However, reducing the flux by 20% is still not enough for the model to match the observations. Other uncertainties in the calculation of the inorganic iodine flux calculation are in the Henry's law of HOI, which has not been measured but is

https://doi.org/10.5194/acp-2020-1219
Preprint. Discussion started: 10 December 2020


Atmospheric Chemistry and Physics Discussions

estimated. Past reports in the Indian Ocean have also questioned the accuracy of the parameterisation-based sea-to-air flux of iodine species in the Indian Ocean (Inamdar et al., 2020; Mahajan et al., 2019a). The current model results also suggest that the accuracy of the flux needs to be revisited, and direct flux observations, which have not been made to date, would be helpful in quantification of the inorganic iodine emissions.

Additionally, there are other sources of uncertainties which could contribute to the mismatch. For example, the treatment of the heterogeneous chemistry has large uncertainties in their uptake coefficients associated to the ability of the model to simulate the aerosol size distribution (and aerosol surface area) and the mixing state and surface composition of the atmospheric aerosols. The photochemistry of I_2O_x species also represents an important source of uncertainty in the iodine chemical mechanism incorporated into chemistry transport models (Lewis et al., 2020; Saiz-Lopez and von Glasow, 2012; Sommariva et al., 2012). However, a new set of I_xO_y photodepletion experiments have recently been reported, but not been incorporated in the available model mechanisms (Lewis et al., 2020). A further uncertainty on the IO concentration calculation is that most chemical transport models tend to underestimate the sources of nitrogen in the open ocean resulting in lower levels of NO_x in the MBL e.g. Travis et al. (2020), which could lead to higher mixing ratios of IO.

Using a reduced flux, seasonally, the highest levels of IO across the domain are observed during the winter monsoon period in January, and the lowest levels are observed during the summer monsoon period in July (Figure 4). While higher values (between 0.7 – 0.9 pptv) are observed in the Bay of Bengal compared to the Arabian Sea, a clear peak in IO is seen close to 3º N in the Western Indian Ocean, between 65º E and 70º E. This high is even more prominent during the pre-monsoon season in April, with the peak monthly averaged values reaching as high as 1.3 pptv. A similar high is also observed during April in the eastern part of the domain close to the equator. A strong seasonal variation is seen, with IO values significantly lower in July as

https://doi.org/10.5194/acp-2020-1219
Preprint. Discussion started: 10 December 2020


Atmospheric Chemistry and Physics Discussions

compared to January and April. July is the summer monsoon period, and is characterised by cleaner air over the domain, with clean oceanic air coming from the south-west (Figure 1). This leads to a reduction in the concentrations of pollutants in the MBL. Considering that the emission of inorganic iodine is driven by the deposition of O_3 at the surface, the reduction in IO can be attributed to a lower concentration of O_3 in the MBL in July (Figure 5). When averaged over the entire domain, the mean IO mixing ratios are 0.47±0.32 pptv in January, 0.48±0.33 pptv in April and 0.15±0.15 pptv in July, showing the strong seasonality driven by the emission of inorganic iodine compounds from the ocean surface. When a land mask is applied and a mean only over the MBL is computed, the values increased to 0.63±0.20 pptv in January, 0.64±0.22 pptv in April and 0.19±0.14 pptv in July. These values are higher than the means across the entire domain, showing that most of the IO is restricted to the MBL, close to the oceanic sources. The concentrations of IO in the current domain are lower than levels predicted by past studies in other environments. Using a similar setup to the current study in WRF-Chem, Badia et al. (2019) estimated IO levels of 0.5 pptv in the subtropics as compared to about 0.8 pptv in the tropics in the MBL. Li et al. (2020) predicted higher levels in the south China Sea, with IO values ranging between 1 – 3 pptv. By comparison, results from the Community Multiscale Air Quality Modelling System (CMAQ) predicted peaks of 4-7 pptv in the coastal regions around Europe, while the open ocean concentrations were below 1 pptv (Li et al., 2019). Thus, in comparison, the values in the Indian Ocean are lower, especially in July, than other regions studied hitherto using regional models, implying a reduced impact of iodine chemistry on the atmosphere in the northern Indian Ocean environment.

The bottom panels in Figure 4 show the difference in IO between the HAL and orgI scenarios. During January and April, the differences are large, with most of the IO being contributed by the inorganic emissions. The largest differences (~1.2 pptv) are observed in locations where a peak is seen in the HAL scenario, closer to the equator. During July, the differences are smaller,

https://doi.org/10.5194/acp-2020-1219
Preprint. Discussion started: 10 December 2020


Atmospheric Chemistry and Physics Discussions

with most of the open ocean MBL showing a smaller increase compared to the other seasons when the inorganic flux is included. It should however be remembered that even though the differences in July are only as high as 0.5 pptv, the orgI scenario predicts only up to 0.04 pptv during this season, which is lower by an order of magnitude. Seasonally also, the difference between the two scenarios is large, with the domain averaged IO mixing ratios showing values of 0.46±0.31 pptv in January, 0.47±0.32 pptv in April and 0.14±0.14 pptv in July for the HAL-orgI contribution. When a land mask is applied and a mean only over the MBL is computed, the values are 0.62±0.20 pptv in January, 0.63±0.21 pptv in April and 0.18±0.14 pptv in July. This suggests that most of the IO in the Indian Ocean MBL is due to emissions of inorganic iodine compounds, rather than the photolysis of organoiodides, which are long-lived and hence do not contribute heavily to the MBL. A similar result has been observed in other oceanic MBLs, where observations show that a small fraction of the total IO in the MBL is due to organic compounds (Mahajan et al., 2010b).

For the rest of the analysis, we use the difference between the HAL and BASE scenarios to quantify the impact of iodine chemistry considering that the orgI greatly underestimates the iodine concentrations in the model domain. The differences and percentage differences in oxidising species such as ozone (O_3), nitrogen oxides (NO_2 and NO), hydrogen oxides (OH and HO_2) and the nitrate radical (NO_3) are studied to quantify the impact of iodine on the MBL atmosphere.

3.3 Impact on ozone

Figure 5 shows the geographical distribution of O_3 across the selected domain during the three seasons for the HAL scenario, along with the absolute and percentage difference between the HAL and BASE scenarios. As expected, much higher concentrations of O_3 are observed over the Indian subcontinent as compared to in the surrounding ocean MBL, with O_3 mixing ratios

https://doi.org/10.5194/acp-2020-1219
Preprint. Discussion started: 10 December 2020


Atmospheric Chemistry and Physics Discussions

peaking over 50 ppbv in the subcontinent as compared to mixing ratios less than 10 ppbv in certain parts of the MBL. A steady decrease is observed from the coast to the open ocean environment, which is expected considering that the main sources of O_3 are emitted on the subcontinent. Seasonal changes are observed, with higher concentrations observed during January and April as compared to the summer monsoon period. During January and April, the winds flow from the subcontinent towards the open ocean, while during July the winds flow from the open ocean towards the subcontinent, which results in cleaner air masses during July (Figure 1). Additionally, during the summer monsoon, wet deposition also plays a role in the removal of O_3 and its precursors from the atmosphere. During January, higher values are observed in the MBL, which is due to stronger winds advecting the polluted air masses from the continent (Figure 1). The model also predicts higher values of O_3 over the Bay of Bengal as compared to the Arabian Sea, which was also seen in the observations (Figure 2). When averaged over the entire domain, the mean O_3 mixing ratios are 32.16±9.76 ppbv in January, 29.64±10.79 ppbv in April, and 23.34±8.85 ppbv in July for the HAL scenario. The lowest values are seen during the monsoon period when cleaner oceanic air is seen over the domain (Table 2). If only the MBL, where elevated concentrations of IO are observed, is considered, the mean O_3 mixing ratios are 28.17±7.83 ppbv in January, 24.17±6.42 ppbv in April, and 19.49±5.97 ppbv in July. This shows that the advection of anthropogenic sources from the continent affects the ozone in the remote MBL too (Table 2).

The middle panels of Figure 5 show the absolute difference in O_3 over the model domain. During January and April significant ozone destruction is observed in the MBL, with as much as 3.5 ppbv lower O_3 in the HAL scenario as compared to the BASE scenario. During January relatively larger destruction is observed in the Bay of Bengal as compared to the Arabian Sea. Significant losses in O_3 are also observed in the western Indian Ocean closer to the equator. Interestingly, O_3 destruction is also visible over the Indian subcontinent, showing that the

https://doi.org/10.5194/acp-2020-1219
Preprint. Discussion started: 10 December 2020


Atmospheric Chemistry and Physics Discussions

effects of iodine chemistry are not just limited to the MBL. In January, an increase of 1 ppbv is seen in over the south of India. During April, the destruction of O_3 is more restricted to the MBL, with larger destruction observed in the Arabian Sea as compared to the Bay of Bengal. The main difference in the O_3 during these two months is driven by the dynamics which dictates where the oceanic emissions of iodine are advected. During July, negligible difference is observed between the HAL and BASE case, with the depletion within ±0.3 ppbv, which reflects the lower concentrations of iodine during the summer monsoon period. When averaged over the entire domain, the mean change in O_3 mixing ratios are -1.20±0.77 ppbv in January, -0.97±0.71 ppbv in April and a small increase of 0.01±0.31 ppbv in July, showing that through January and April a mean reduction is observed, but in July there is a statistically non-significant increase when the IO concentrations are very low. This change in ozone is mainly driven by changes in the MBL, where the differences are -1.31±0.67 ppbv in January, -1.22±0.65 ppbv in April and -0.10±0.21 ppbv in July. If we consider the absolute changes rather than the mean change, the average over the whole domain is larger at 1.25±0.69 ppbv in January, 0.98±0.69 ppbv in April and 0.21±0.22 ppbv in July, while over the MBL the differences are 1.31±0.66 ppbv in January, 1.22±0.65 ppbv in April and 0.15±0.18 ppbv in July (Table 3). The reason for larger absolute differences as compared to mean differences is that there are both increases and decreases seen through the domain, and hence the absolute differences gives us an idea of the total impact of iodine chemistry.

The bottom panels in Figure 5 show the percentage change in O_3 between the BASE and HAL scenarios. As much as 20% reduction in the O_3 concentrations is observed in the MBL when iodine chemistry is included, with the largest differences observed in the western part of the domain, closer to the equator. For most of the domain, the change in O_3 is <15%. Over the Indian subcontinent, and close to the coastal areas, the relative change in O_3 is small, which is due to larger absolute concentrations in these locations. In January and July, a small increase

https://doi.org/10.5194/acp-2020-1219
Preprint. Discussion started: 10 December 2020


Atmospheric Chemistry and Physics Discussions

(<5%) in the O_3 concentrations is predicted over large parts of the domain. This shows the non-linear effect of iodine chemistry on the atmosphere, which can lead to an increase in O_3 in certain parts of the domain due to changes in other oxidants. When averaged over the entire domain, the mean percentage changes in O_3 mixing ratios are -3.60±3.33 % in January, -3.16±3.62 % in April and 0.06±1.37 % in July, showing that the largest relative change is seen during the winter period in January followed by the pre-monsoon season in April, while the smallest change is in July during the monsoon when the IO values are low (Table 2). Over the MBL, the mean percentage changes in O_3 mixing ratios are -4.43±3.39 % in January, -4.80±3.49 % in April, and -0.51±1.26 in July, which means that larger differences are seen in the MBL rather than over the Indian subcontinent (Table 2). When the absolute change is computed, the differences are similar with the average over the whole domain showing a 3.75±3.17 % change in January, 3.21±3.58 % change in April and 0.89±1.04 % change in July, and only over the MBL, the absolute percentage change is 4.45±3.37 % in January, 4.80±3.49 % in April and 0.77±1.13 % in July (Table 3). The fact that the absolute change values are close to the mean change values shows that most of the domain sees a destruction in ozone due to the presence of iodine compounds.

This relative change is lower than in the Pacific, where the WRF-Chem simulated O_3 destruction because of all halogens peaked at -16 ppbv, which was approximately 70% of the total ozone loss, of which 18-23% was because of iodine chemistry (Badia et al., 2019). The loss of O_3 due to iodine was similar to the current domain in China, where the range of ozone destruction/production because of all halogens was -10 to +5% (Li et al., 2020). Over Europe, combined halogen chemistry, which includes I, Br and Cl, significantly reduces the concentrations of and O_3 by as much as 10 ppbv. The contribution because of only iodine is also larger than in the current domain, which is expected because of the higher IO concentrations simulated in Europe (Li et al., 2019).

https://doi.org/10.5194/acp-2020-1219
Preprint. Discussion started: 10 December 2020

Atmospheric Chemistry and Physics Discussions

3.4 Impact on nitrogen oxides (NO_x)

Halogen oxides interact with nitrogen oxides to change the NO/NO_2 ratio by reacting with NO to form NO_2. Additionally, iodine oxides can also react with NO_x to form iodine nitrate ($IONO_2$), which can be taken up on aerosol surfaces to act as a sink or recycle both nitrogen compounds and iodine compounds (Atkinson et al., 2007). Thus, the resultant increase or decrease in nitrogen oxides depends on the concentrations of iodine compounds, concentrations of nitrogen compounds and the aerosol surface available for heterogenous recycling. Figures 6 and 7 show the geographical distribution of NO_2 and NO across the selected domain during the three seasons, for the HAL scenario, along with the absolute and percentage difference between the HAL and BASE scenarios. As expected, much higher concentrations of NO_2 are observed over the Indian subcontinent as compared to the surrounding ocean MBL, with NO_2 mixing ratios peaking over 5 ppbv in the subcontinent as compared to mixing ratios less than 0.2 ppbv in certain parts of the MBL (Figure 6). The hotspots for NO_2, which are either power plants or large cities, are clearly visible. A sharp decrease is observed from the coast to the open ocean environment, which is expected considering that the primary sources of NO_2 are on the subcontinent. The shipping lanes in the Indian Ocean also show higher concentrations of NO_2, and are clearly visible, especially south of the Indian subcontinent, where NO_2 mixing ratios of up to 1 ppbv can be seen. A seasonal variation is also observed, with higher concentrations observed during winter in January, followed by the pre-monsoon period in April, with the summer monsoon period in July showing the lowest concentrations, even at the hotspots. When averaged over the entire domain, the mean NO_2 mixing ratios are 0.43±1.27 ppbv in January, 0.30±0.77 ppbv in April, and 0.27±0.79 in July for the HAL scenario, with the lowest values observed during the monsoon period when cleaner oceanic air is seen over the domain (Table 2). Over only the MBL, the mean NO_2 mixing ratios are 0.10±0.46 ppbv in January, 0.06±0.30

https://doi.org/10.5194/acp-2020-1219
Preprint. Discussion started: 10 December 2020


Atmospheric Chemistry and Physics Discussions

ppbv in April, and 0.07±0.29 ppbv in July. This shows that the MBL is much cleaner than the air above the Indian subcontinent (Table 2).

Similar to NO_2, NO also shows higher concentrations over the Indian subcontinent as compared to the surrounding ocean MBL, with NO mixing ratios peaking over 400 pptv in the subcontinent as compared to mixing ratios less than 20 pptv in large parts of the MBL (Figure 7). The hotspots for NO, which coincide with the hotspots for NO_2, are also clearly visible. A sharp decrease is observed from the coast to the open ocean environment like NO_2, indicating that fossil fuel combustion over land is the main source. The shipping lanes in the Indian Ocean are more noticeable than for NO_2, with NO mixing ratios of up to 200 pptv observed in some regions. The seasonal variation for NO follows the same trend as NO_2, with higher concentrations observed during January, followed by April, with the summer monsoon period in July showing the lowest concentrations. However, January shows the lowest concentrations in the shipping lanes. When averaged over the entire domain, the mean NO mixing ratios are 49.50±221.23 pptv, 36.66±164.95 pptv and 38.79±173.78 pptv in January, April, and July, respectively (Table 2). The large standard deviations show that the high concentrations of NO are mainly restricted to hotspots. Over only the MBL, the mean NO_2 mixing ratios are 12.56±85.76 pptv in January, 10.38±77.48 pptv in April, and 11.64±58.45 pptv in July. The lower values and the smaller standard deviations show that the MBL is much cleaner than the air above the Indian subcontinent and does not contain large hotspots although it is affected by the coastal regions (Table 2).

The middle panels of Figures 6 and 7 show the absolute difference in NO_2 and NO for the HAL and BASE scenarios. For NO_2, a small reduction is observed in most of the MBL during all the months, with changes of about -0.04 ppbv observed at most locations. Over the subcontinent, there is variation observed at some locations, with decreases and increases showing a maximum of ±0.08 ppbv. Over the shipping lanes, where high NO_2 is observed, an increase of about 0.04

https://doi.org/10.5194/acp-2020-1219
Preprint. Discussion started: 10 December 2020


Atmospheric Chemistry and Physics Discussions

ppbv is observed after the inclusion of iodine chemistry. In the case of NO, the variation observed is similar to NO_2, with a small reduction observed in most of the MBL during all the months, with changes of about -2 pptv observed at most locations. Over the subcontinent, significant variation is also observed for NO, with decreases and increases showing a maximum of ±8 pptv. In most of the shipping lanes, where high NO is observed, the inclusion of iodine chemistry leads to an increase in the NO_x concentrations, especially in April, where the increase in NO_2 can be as high as ~10% and the increase in NO can be as high as 15%. When averaged over the whole domain, the mean change in NO_2 mixing ratios is negligible at -0.0040±0.0209 ppbv in January, 0.0007±0.0195 ppbv in April and 0.0003±0.0129 ppbv in July. Over the MBL too, the differences are just -0.0025±0.0071 ppbv in January, -0.0005±0.0070 ppbv in April and -0.0008±0.0061 ppbv in July (Table 2). This is because NO_2 shows an increase in some regions within the domain and a decrease in other parts. In the case of NO, the average difference over the whole domain is also small at -0.23±5.83 pptv in January, 0.59±6.49 pptv in April and -0.09±4.44 pptv in July. Over the MBL too, the differences are just -0.25±2.85 pptv in January, 0.16±2.87 pptv in April and -0.20±1.99 in July (Table 2). However, similar to NO_2, these values are misrepresentative of the effect of IO because of differences in the sign of the change across the domain. If we consider the mean absolute difference instead of just the mean difference, the larger impact of iodine chemistry can be discerned, with a mean absolute difference in the NO_2 mixing ratios of 0.008±0.019 ppbv in January, 0.007±0.018 ppbv in April and 0.004±0.012 ppbv in July across the whole domain and 0.004±0.007 ppbv in January, 0.002±0.007 ppbv in April and 0.002±0.006 ppbv in July only over the MBL. For NO, the change is also higher at 1.60±5.61 pptv in January, 1.57±6.33pptv in April and 1.03±4.32 pptv in July across the whole domain and 0.70±2.78 pptv, 0.72±2.78 pptv and 0.45±1.95 pptv in only the MBL during January, April and July (Table 3).

https://doi.org/10.5194/acp-2020-1219
Preprint. Discussion started: 10 December 2020


Atmospheric Chemistry and Physics Discussions

456 The bottom panels in Figures 6 and 7 show the percentage changes in NO_2 and NO between
457 the BASE and HAL scenarios. Significant differences are observed over the MBL with
458 decreases in NO_x as high as 50% over large areas when iodine chemistry is included. The
459 largest differences are observed in the western Arabian Sea and in the southern Bay of Bengal.
460 Over the Indian subcontinent, and close to the coastal areas, the relative change in both NO_2
461 and NO is small, due to larger absolute concentrations in these locations, although a small
462 increase is observed over most of the land area. In the shipping lanes, NO_x mostly shows an
463 increase, which is due to the recycling of halogen nitrates on the aerosol surfaces. When
464 averaged over the whole domain, the mean percentage change in NO_2 mixing ratios is small at
465 -0.91±11.08 %, 0.22±6.89 % and 0.1±5.85 % in January, April, and July. Over the MBL, mean
466 values of the differences are slightly higher with values of -2.42±11.62 %, -0.91±7.19 % and -
467 1.19±6.24 % in January, April, and July. This suggests that the inclusion of iodine chemistry
468 leads to the reduction in NO_2 in the domain, albeit with a large variation, which would
469 contribute to the reduction in O_3 as mentioned above since NO_2 is the main source of ozone in
470 the MBL. The change in NO is also small at -0.47±15.32 % in January, 1.64±10.85 % in April
471 and -0.23±7.35 % in July, with slightly higher values observed when averaged only over the
472 MBL: 1.96±15.6 % in January, 1.54±11.60 % in April and -1.71±7.73 in July (Table 2). When
473 we consider the mean absolute change to see the actual impact of iodine chemistry, the values
474 of the means are much higher, with as much as ~3.5% change in NO_2 and 7% change in NO
475 observed over the MBL (Table 3). This change in NO_x is smaller than simulated in Europe with
476 NO_2 predicted to increase across most of Europe with most regions showing an increase
477 between 50 – 200 pptv. However, this was the increase reported due to the inclusion of all the
478 halogens, and the impact of only iodine would be lower, even though higher levels were
479 simulated across Europe (Li et al., 2019).

480

https://doi.org/10.5194/acp-2020-1219
Preprint. Discussion started: 10 December 2020

Atmospheric Chemistry and Physics Discussions

3.5 Impact on hydrogen oxides (HO_x)

Hydrogen oxides are impacted by iodine chemistry through the catalytic reaction involving IO changing HO_2 into OH. This leads to an increase in the oxidizing capacity of the atmosphere due to an increase in the OH concentrations. Figures 8 and 9 show the geographical distribution of OH and HO_2 across the selected domain during the three seasons for the HAL scenario, along with the absolute and percentage differences between the HAL and BASE scenarios. The daily averaged OH mixing ratios peak at about 0.5 pptv in the MBL close to the Indian subcontinent, as compared to mixing ratios less than 0.3 pptv over most of the subcontinent (Figure 8). The shipping lanes in the Indian Ocean show higher concentrations of OH, and are clearly visible, especially south of the Indian subcontinent and in the Arabian Sea, where OH mixing ratios of up to 0.45 pptv can be seen. A strong seasonal variation is observed as expected, with higher concentrations observed during the months of April and July, with the winter period in January showing the lowest concentrations. This annual variation is driven by the availability of solar radiation, which is a critical component in OH production. When averaged over the entire domain, the mean OH mixing ratios are 0.14±0.05 pptv, 0.26±0.07 pptv and 0.28±0.08 pptv in January, April, and July, respectively (Table 2). Over only the MBL, the mean OH mixing ratios are 0.15±0.05 pptv in January, 0.27±0.08 pptv in April and 0.27±0.08 pptv in July (Table 2).

HO_2 shows much higher concentrations over the Indian subcontinent as compared to the surrounding ocean MBL, with HO_2 mixing ratios peaking over 15 pptv in the subcontinent as compared to mixing ratios less than 10 pptv over most of the MBL (Figure 9). There is a correlation between the hotspots for NO_x, and low concentrations of HO_2 over the Indian subcontinent. This is due to the titration of HO_2 by NO, which forms NO_2 and leads to an increase in O_3 formation. A gradual decrease in the HO_2 mixing ratios is observed from the subcontinent to the open ocean environment during the months of April and July, although the

https://doi.org/10.5194/acp-2020-1219
Preprint. Discussion started: 10 December 2020


Atmospheric Chemistry and Physics Discussions

506 HO_2 concentrations in the MBL are larger during January. Relatively, the winter month of
507 January shows the lowest HO_2 mixing ratios of the three months. The shipping lanes in the
508 Indian Ocean are clearly visible like for OH, although the HO_2 concentrations in the shipping
509 lanes are lower than the surrounding areas. This is due to the earlier mentioned titration of HO_2
510 by ship emitted NO, which leads to an increase in OH but a decrease in HO_2. When averaged
511 over the entire domain, the mean HO_2 mixing ratios are 7.10±1.49 pptv, 10.18±1.64 pptv and
512 9.24±1.97 pptv in January, April, and July, respectively (Table 2). Over only the MBL, the
513 mean HO_2 mixing ratios are higher at 7.32±1.12 pptv, in January but lower in April and July
514 at 9.80±1.36 and 8.67±1.53 pptv (Table 2).

515 The middle panels of Figures 8 and 9 show the absolute difference in OH and HO_2. For OH, a
516 small increase in the OH concentration is observed in most of the MBL during the months of
517 January and April, with the largest increase of about 0.03 pptv observed in the Arabian Sea.
518 However, for most of the domain, the increase in OH is small, with differences of 0.01 pptv
519 compared to the BASE scenario. During the monsoon month of July, a small decrease is
520 observed over most of the domain with an increase observed further south close to the equator.
521 Over the shipping lanes, a small reduction is observed during all the months, with changes of
522 about -0.02 pptv along the ship tracks. In the case of HO_2, a clear land ocean contrast is
523 observed in the differences, with the HO_2 values reducing over the entire MBL, but showing a
524 small increase over the subcontinent. The largest reduction is observed in the south-western
525 Arabian Sea, with changes of about -1.8 pptv in the HAL scenario as compared to the BASE
526 case. Seasonally, the largest changes in HO_2 are observed in January, with the least changes
527 observed in the monsoon month of July. IO concentrations are the lowest during monsoon due
528 to clean air-masses reducing the ozone deposition driven emissions and hence the difference
529 between the HAL and BASE scenarios is also the lowest during July. When averaged over the
530 whole domain, the mean change in OH mixing ratios is negligible at 0.001±0.006 pptv in

https://doi.org/10.5194/acp-2020-1219
Preprint. Discussion started: 10 December 2020


Atmospheric Chemistry and Physics Discussions

January, 0.006±0.007 pptv in April and -0.003±0.006 in July. In the case of HO_2, the average difference over the whole domain is also small at -0.48±0.43 pptv in January, -0.35±0.38 pptv in April and -0.19±0.16 in July. Over the MBL too, the differences are larger with the largest difference being -0.67±0.36 pptv in January (Table 2).

The bottom panels in Figures 8 and 9 show the percentage changes in OH and HO_2 between the BASE and HAL scenarios. Significant differences are observed with an increase in OH and a decrease in the HO_2 over most of the MBL. The largest change in OH is observed in the northern Arabian Sea MBL, with a difference of more than 15% between the HAL and BASE cases when iodine chemistry is included. Large parts of the Arabian Sea and the Bay of Bengal show an increase in OH of up to 10% for January and April, with a smaller difference observed in July due to lower concentrations of iodine compounds in the atmosphere. In January and April, when the concentrations of IO are higher, a negative change in the OH concentrations are observed over the shipping lanes. In the case of HO_2, a large change of up to 25% is observed in the MBL, with the largest differences observed in the southern western Arabian Sea, close to the equator. During the months of January and April, most of the MBL shows a change of -10 to -20 %, while a positive change of 0-5% is observed over the Indian subcontinent. The mean percentage change in the OH and HO_2 mixing ratios peaks at 2.6 % and 8.4 % for the months of April and July, respectively (Table 2), but the absolute percentage change in OH is higher at 3.6 % in January, while the HO_2 absolute percentage change (Table 3) is about ~8.4 % showing the large impact of iodine chemistry on the oxidation capacity of the MBL. For example, the 3.29% increase in the OH concentrations observed across the domain in January would result in the lowering of the methane lifetime by 3.19% in the MBL (assuming $k_{CH4+OH} = 1.85\times10^{-12}\exp(-1690/T)$; (Atkinson et al., 2006)). A similar change in the oxidizing capacity has been simulated in other parts of the world, with halogen chemistry inducing complex effects on OH (ranging from −0.023 to 0.030 pptv) and HO_2 (in the range of

https://doi.org/10.5194/acp-2020-1219
Preprint. Discussion started: 10 December 2020


Atmospheric Chemistry and Physics Discussions

556 −3.7 to 0.73 pptv) in Europe (Li et al., 2019) and enhancing the total atmospheric oxidation
557 capacity in polluted areas of China, typically 10% to 20% (up to 87% in winter) and mainly by
558 significantly increasing OH levels (Li et al., 2020). The moderate increase in the oxidation
559 capacity over the northern Indian Ocean and the Indian subcontinent is due to the lower
560 concentrations of IO in the domain, along with the fact that this number is calculated only for
561 the impact of iodine chemistry, while the past studies have reported the impact of all halogens.
562 Globally the average increase in OH because of the inclusion of iodine chemistry has been
563 estimated to be 1.8 %, which is comparable to the current domain (Sherwen et al., 2016).

564

565 **3.6 Impact on the nitrate radical (NO_3)**

566 NO_3 radicals are the predominant night-time oxidant and play a similar role to OH during the
567 daytime in the degradation of atmospheric constituents (Wayne et al., 1991). Iodine compounds
568 interact with NO_3, mainly through the primary emissions of inorganic iodine compounds by
569 the oxidation of chemicals such as I_2 and HOI (Saiz-Lopez et al., 2016). Figure 10 shows the
570 geographical distribution of NO_3 across the selected domain during the three seasons, for the
571 HAL scenario, along with the absolute and percentage difference between the HAL and BASE
572 scenarios. As expected, much higher concentrations of NO_3 are observed over the Indian
573 subcontinent as compared to the surrounding ocean MBL, with NO_3 mixing ratios peaking over
574 40 pptv in the subcontinent as compared to mixing ratios less than 5 pptv in the MBL
575 surrounding the Indian subcontinent. A sharp decrease is observed from the coast to the open
576 ocean environment, which is expected considering that the main sources of NO_3 are on the
577 subcontinent and NO_3 has a short lifetime due to its high reactivity. The seasonal variation is
578 the same as O_3, with peak values observed over the Indian subcontinent over the month of
579 April, followed by January. The monsoon month of July displays the lowest concentrations,

https://doi.org/10.5194/acp-2020-1219
Preprint. Discussion started: 10 December 2020


Atmospheric Chemistry and Physics Discussions

due to efficient removal of NO_x and O_3 due to wet deposition. Elevated values up to 15 pptv are also observed along the shipping lanes due to the conversion of ship emitted NO_x into NO_3 during the night-time. When averaged over the entire domain, the mean NO_3 mixing ratios are 7.64±8.08 pptv in January, 10.38±15.53 pptv in April and 4.52±6.14 pptv in July for the HAL scenario. The lowest values are observed during the monsoon period similar to O_3 when cleaner oceanic air is observed over the domain (Table 2). If only the MBL, where lower concentrations of NO_x are observed is considered, the mean NO_3 mixing ratios are 4.47±5.44 pptv in January, 2.99±4.09 pptv in April, and 2.38±3.94 pptv in July (Table 2).

The middle panels of Figure 10 show the absolute difference in NO_3 over the model domain. During the months of January and April, a significant reduction of up to -1.5 pptv is observed in the MBL. During January, a reduction is observed in the Bay of Bengal as well as the Arabian Sea, but in April the reduction in NO_3 is largely observed in the Arabian Sea. This correlates well with the IO distribution which also shows more iodine activity in the Arabian Sea during April. A reduction in NO_3 is also visible over the Indian subcontinent, and like O_3 show that the effects of iodine chemistry are not just limited to the MBL. Indeed, there are pockets of an increase in NO_3 observed over the subcontinent. During July, negligible difference is observed between the HAL and BASE case, with a smaller than 0.5 pptv decrease seen across the MBL. However, during the same period, an increase of up to 1.5 pptv can be seen over the NO_x hotspots over the Indian subcontinent. Decreases of up to -1.5 pptv are also observed along the shipping lanes, showing the strong interaction between iodine and NO_x chemistry. Over the whole domain, the inclusion of iodine chemistry results in a mean decrease of about ~-0.4 pptv, which is slightly higher when a mean is taken only for the MBL (Table 2). The absolute change in NO_3 is even higher, with NO_3 values changing by an average of 0.5 pptv across the whole domain in July (Table 3). This value is however lower than the effect of all the halogens, as

https://doi.org/10.5194/acp-2020-1219
Preprint. Discussion started: 10 December 2020


Atmospheric Chemistry and Physics Discussions

shown by Li et al. (2019) in Europe, where halogens significantly reduced the concentrations of NO_3 by as much as 20 pptv.

The bottom panels in Figure 10 show the percentage change in NO_3 between the BASE and HAL scenarios. As much as a 50% reduction in the NO_3 concentrations is observed in the MBL when iodine chemistry is included, with the largest differences observed in the Arabian Sea, close to the Indian subcontinent, further west closer to the equator and in the Bay of Bengal. For most of the other domain, the change in NO_3 is <20%. Over the Indian subcontinent, the relative change in NO_3 is small, due to larger absolute concentrations and in some places a small increase (<5%) is predicted, especially in July when iodine chemistry is not highly active. The relative change in the shipping lanes is smaller than the surrounding areas due to the higher relative concentrations of NO_3 along the tracks (<20%). On average, the inclusion of iodine chemistry can cause an almost 10% change in the NO_3 concentrations across the MBL in January with smaller changes of ~4.5% observed during July when the IO concentrations are lower (Table 3).

4. Conclusions

In this study, we used the WRF-Chem regional model to quantify the impacts of the observed levels of iodine on the chemical composition of the MBL over the northern Indian Ocean. The model results show that the IO concentrations are greatly underestimated if only organic iodine compound emissions are considered in the model. This reaffirms that emissions of inorganic species resulting from the deposition of ozone on the sea surface are needed to reproduce the observed levels of IO. However, the current parameterisations overestimate the concentrations, which could be because of a combination of modelling uncertainties and the HOI and I_2 flux parameterisation not being directly applicable to this region. This agrees with previous reports

https://doi.org/10.5194/acp-2020-1219
Preprint. Discussion started: 10 December 2020


Atmospheric Chemistry and Physics Discussions

628 in the Indian Ocean questioning the current parameterisations and highlights the need for direct
629 HOI and I_2 flux observations. For a reasonable match with cruise-based observations, the
630 inorganic emissions had to be reduced by 40%. The simulations after this reduction in flux
631 show a strong seasonal variation, with lower iodine concentrations predicted when cleaner air
632 is found over the Indian subcontinent due to flushing by remote oceanic air masses during the
633 monsoon season but higher iodine concentrations are predicted during the winter period, when
634 polluted air from the Indian subcontinent increases the ozone concentrations in the MBL. A
635 large regional variation is observed in the IO distribution, and also in the impacts of iodine
636 chemistry. Iodine catalysed reactions can lead to significant regional changes with peaks of
637 25% destruction in O_3, altering the NOx concentrations by up to 50%, increasing the OH
638 concentration by as much as 15%, reducing the HO_2 concentration by as much as 25%, and up
639 to a 50% change in the nitrate radical (NO_3). When averaged across the whole domain, the
640 differences are smaller, although still significant. For example, the average change in OH
641 across the whole domain reduces the methane lifetime by ~3% in the MBL showing the impact
642 of iodine on the oxidation capacity. Most of the large relative changes are observed in the open
643 ocean MBL but iodine chemistry also affects the chemical composition in the coastal
644 environment and over the Indian subcontinent. Indeed, in some instances an increase in O_3
645 concentrations is predicted over the subcontinent, showing the non-linear effects. These model
646 results highlight the importance of iodine chemistry in the northern Indian Ocean and suggest
647 that it needs to be included in future studies for improved accuracy in modelling the chemical
648 composition in this region.

649

650 **Acknowledgements**

https://doi.org/10.5194/acp-2020-1219
Preprint. Discussion started: 10 December 2020


Atmospheric Chemistry and Physics Discussions

IITM is funded by the Ministry of Earth Sciences (MOES), Government of India. This study has been funded by the European Research Council Executive Agency under the European Union´s Horizon 2020 Research and Innovation programme (Project 'ERC-2016-COG 726349 CLIMAHAL').

Author Contributions

ASM conceptualized the research plan and methodology, analysed the data, and wrote the paper. QL did the model runs for the study and contributed towards the interpretation of the results and writing. SI helped with the analysis, interpretation and writing. KR, AB and ASL contributed towards the interpretation and writing.

Competing interests

The authors declare that they have no conflict of interest.

References

Alicke, B., Hebestreit, K., Stutz, J. and Platt, U.: Iodine oxide in the marine boundary layer, Nature, 397(6720), 572–573, doi:10.1038/17508, 1999.

Allan, B. J., McFiggans, G., Plane, J. M. C. and Coe, H.: Observations of iodine monoxide in the remote marine boundary layer, J. Geophys. …, 105(D11), 14363–14369 [online] Available from: http://onlinelibrary.wiley.com/doi/10.1029/1999JD901188/full (Accessed 18 August 2014), 2000.

Allan, J. D., Williams, P. I., Najera, J., Whitehead, J. D., Flynn, M. J., Taylor, J. W., Liu, D.,

https://doi.org/10.5194/acp-2020-1219
Preprint. Discussion started: 10 December 2020


Atmospheric Chemistry and Physics Discussions

673 Darbyshire, E., Carpenter, L. J., Chance, R., Andrews, S. J., Hackenberg, S. C. and
674 McFiggans, G.: Iodine observed in new particle formation events in the Arctic atmosphere
675 during ACCACIA, Atmos. Chem. Phys., 15(10), 5599–5609, doi:10.5194/acp-15-5599-2015,
676 2015.

677 Atkinson, R., Baulch, D. L., Cox, R. A., Crowley, J. N., Hampson, R. F., Hynes, R. G.,
678 Jenkin, M. E., Rossi, M. J., Troe, J. and Wallington, T. J.: Evaluated kinetic and
679 photochemical data for atmospheric chemistry: Volume IV -- gas phase reactions of organic
680 halogen species, Atmos. Chem. Phys., 6, 1461–1738, 2006.

681 Atkinson, R., Baulch, D. L., Cox, R. A., Crowley, J. N., Hampson, R. F., Hynes, R. G.,
682 Jenkin, M. E., Rossi, M. J. and Troe, J.: Evaluated kinetic and photochemical data for
683 atmospheric chemistry: Volume III - gas phase reactions of inorganic halogens, Atmos.
684 Chem. Phys., 7(4), 981–1191, 2007.

685 Baccarini, A., Karlsson, L., Dommen, J., Duplessis, P., Vüllers, J., Brooks, I. M., Saiz-Lopez,
686 A., Salter, M., Tjernström, M., Baltensperger, U., Zieger, P. and Schmale, J.: Frequent new
687 particle formation over the high Arctic pack ice by enhanced iodine emissions, Nat.
688 Commun., 11(1), 1–11, doi:10.1038/s41467-020-18551-0, 2020.

689 Badia, A., Reeves, C. E., Baker, A. R., Saiz-Lopez, A., Volkamer, R., Koenig, T. K., Apel, E.
690 C., Hornbrook, R. S., Carpenter, L. J., Andrews, S. J., Sherwen, T. and Glasow, R. von:
691 Importance of reactive halogens in the tropical marine atmosphere: A regional modelling
692 study using WRF-Chem, Atmos. Chem. Phys., 19, 3161–3189, doi:10.5194/acp-19-3161-
693 2019, 2019.

694 Bloss, W. J., Lee, J. D., Johnson, G. P., Sommariva, R., Heard, D. E., Saiz-Lopez, A., Plane,
695 J. M. C., McFiggans, G., Coe, H., Flynn, M., Williams, P., Rickard, A. R. and Fleming, Z. L.:
696 Impact of halogen monoxide chemistry upon boundary layer OH and HO2 concentrations at a

https://doi.org/10.5194/acp-2020-1219
Preprint. Discussion started: 10 December 2020


Atmospheric Chemistry and Physics Discussions

697 coastal site, Geophys. Res. Lett., 32(6), 1–4, doi:10.1029/2004GL022084, 2005.

698 Carpenter, L. J.: Iodine in the marine boundary layer, Chem. Rev., 103(12), 4953–4962,
699 doi:Doi 10.1021/Cr0206465, 2003.

700 Carpenter, L. J., MacDonald, S. M., Shaw, M. D., Kumar, R., Saunders, R. W., Parthipan, R.,
701 Wilson, J. and Plane, J. M. C.: Atmospheric iodine levels influenced by sea surface emissions
702 of inorganic iodine, Nat. Geosci., 6(2), 108–111, doi:10.1038/ngeo1687, 2013.

703 Chameides, W. L. and Davis, D. D.: Iodine: Its possible role in tropospheric photochemistry,
704 J. Geophys. Res., 85(C15), 7383–7398, doi:10.1029/JC085iC12p07383, 1980.

705 Chance, R., Tinel, L., Sherwen, T., Baker, A., Bell, T., Brindle, J., Campos, M. L. A. M.,
706 Croot, P., Ducklow, H., He, P., Hoogakker, B., Hopkins, F. E., Hughes, C., Jickells, T.,
707 Loades, D., Macaya, D. A., Mahajan, A. S., Malin, G., Phillips, D. P., Sinha, A. K., Sarkar,
708 A., Roberts, I. J., Roy, R., Song, X., Winklebauer, H. A., Wuttig, K., Yang, M., Zhou, P. and
709 Carpenter, L. J.: Global sea-surface iodide observations, 1967-2018, Nat. Sci. Data, 6(286),
710 doi:doi.org/10.1038/s41597-019-0288-y, 2019.

711 Chance, R., Tinel, L., Sarkar, A., Sinha, A. K., Mahajan, A. S., Chacko, R., Sabu, P., Roy, R.,
712 Jickells, T. D., Stevens, D. P., Wadley, M. and Carpenter, L. J.: Surface Inorganic Iodine
713 Speciation in the Indian and Southern Oceans From 12°N to 70°S, Front. Mar. Sci., 7(621),
714 1–16, doi:10.3389/fmars.2020.00621, 2020.

715 Commane, R., Seitz, K., Bale, C. S. E., Bloss, W. J., Buxmann, J., Ingham, T., Platt, U.,
716 Pöhler, D. and Heard, D. E.: Iodine monoxide at a clean marine coastal site: observations of
717 high frequency variations and inhomogeneous distributions, Atmos. Chem. Phys., 11(13),
718 6721–6733, doi:10.5194/acp-11-6721-2011, 2011.

719 Cuevas, C. A., Maffezzoli, N., Corella, J. P., Spolaor, A., Vallelonga, P., Kjær, H. A.,

https://doi.org/10.5194/acp-2020-1219
Preprint. Discussion started: 10 December 2020

720 Simonsen, M., Winstrup, M., Vinther, B., Horvat, C., Fernandez, R. P., Kinnison, D.,
721 Lamarque, J.-F., Barbante, C. and Saiz-Lopez, A.: Rapid increase in atmospheric iodine
722 levels in the North Atlantic since the mid-20th century, Nat. Commun., 9(1), 1452,
723 doi:10.1038/s41467-018-03756-1, 2018.

724 Furneaux, K. L., Whalley, L. K., Heard, D. E., Atkinson, H. M., Bloss, W. J., Flynn, M. J.,
725 Gallagher, M. W., Ingham, T., Kramer, L. J., Lee, J. D., Leigh, R. J., McFiggans, G. B.,
726 Mahajan, A. S., Monks, P. S., Oetjen, H., Plane, J. M. C. and Whitehead, J. D.:
727 Measurements of iodine monoxide at a semi polluted coastal location, Atmos. Chem. Phys.,
728 10(8), 3645–3663 [online] Available from: http://www.atmos-chem-phys.net/10/3645/2010/,
729 2010.

730 Gómez Martín, J. C., Mahajan, A. S., Hay, T. D., Prados-Román, C., Ordóñez, C.,
731 MacDonald, S. M., Plane, J. M. C., Sorribas, M., Gil, M., Paredes Mora, J. F., Agama Reyes,
732 M. V., Oram, D. E., Leedham, E. and Saiz-Lopez, A.: Iodine chemistry in the eastern Pacific
733 marine boundary layer, J. Geophys. Res. Atmos., 118(2), 887–904, doi:10.1002/jgrd.50132,
734 2013.

735 Großmann, K., Frieß, U., Peters, E., Wittrock, F., Lampel, J., Yilmaz, S., Tschritter, J.,
736 Sommariva, R., von Glasow, R., Quack, B., Krüger, K., Pfeilsticker, K. and Platt, U.: Iodine
737 monoxide in the Western Pacific marine boundary layer, Atmos. Chem. Phys., 13, 3363–
738 3378, doi:10.5194/acp-13-3363-2013, 2013.

739 Iglesias-Suarez, F., Kinnison, D. E., Rap, A., Maycock, A. C., Wild, O. and Young, P. J.:
740 Key drivers of ozone change and its radiative forcing over the 21st century, Atmos. Chem.
741 Phys., 18(9), 6121–6139, doi:10.5194/acp-18-6121-2018, 2018.

742 Inamdar, S., Tinel, L., Chance, R., Carpenter, L. J., Sabu, P., Chacko, R., Tripathy, S. C.,
743 Kerkar, A. U., Sinha, A. K., Bhaskar, P. V., Sarkar, A., Roy, R., Sherwen, T. T., Cuevas, C.,

https://doi.org/10.5194/acp-2020-1219
Preprint. Discussion started: 10 December 2020

Atmospheric Chemistry and Physics Discussions

744 Saiz-Lopez, A., Ram, K. and Mahajan, A. S.: Estimation of Reactive Inorganic Iodine Fluxes
745 in the Indian and Southern Ocean Marine Boundary Layer, Atmos. Chem. Phys., 20(20),
746 12093–12114, doi:10.5194/acp-20-12093-2020, 2020.

747 Lawrence, M. G. and Lelieveld, J.: Atmospheric pollutant outflow from southern Asia: A
748 review, Atmos. Chem. Phys., 10(22), 11017–11096, doi:10.5194/acp-10-11017-2010, 2010.

749 Legrand, M., McConnell, J. R., Preunkert, S., Arienzo, M., Chellman, N., Gleason, K.,
750 Sherwen, T., Evans, M. J. and Carpenter, L. J.: Alpine ice evidence of a three-fold increase in
751 atmospheric iodine deposition since 1950 in Europe due to increasing oceanic emissions,
752 Proc. Natl. Acad. Sci., 115(48), 12136–12141, doi:10.1073/pnas.1809867115, 2018.

753 Lelieveld, J., Crutzen, P. J., Ramanathan, V., Andreae, M. O., Brenninkmeijer, C. A. M.,
754 Campos, T., Cass, G. R., Dickerson, R. R., Fischer, H., De Gouw, J. A., Hansel, A.,
755 Jefferson, A., Kley, D., De Laat, A. T. J., Lal, S., Lawrence, M. G., Lobert, J. M., Mayol-
756 Bracero, O. L., Mitra, A. P., Novakov, T., Oltmans, S. J., Prather, K. A., Reiner, T., Rodhe,
757 H., Scheeren, H. A., Sikka, D. and Williams, J.: The Indian Ocean Experiment: Widespread
758 air pollution from South and Southeast Asia, Science (80-.)., 291(5506), 1031–1036,
759 doi:10.1126/science.1057103, 2001.

760 Lewis, T. R., Gómez Martín, J. C., Blitz, M. A., Cuevas, C. A., Plane, J. M. C. and Saiz-
761 Lopez, A.: Determination of the absorption cross sections of higher-order iodine oxides at
762 355 and 532 nm, Atmos. Chem. Phys., 20(18), 10865–10887, doi:10.5194/acp-20-10865-
763 2020, 2020.

764 Li, Q., Borge, R., Sarwar, G., de la Paz, D., Gantt, B., Domingo, J., Cuevas, C. A. and Saiz-
765 Lopez, A.: Impact of halogen chemistry on summertime air quality in coastal and continental
766 Europe: application of the CMAQ model and implications for regulation, Atmos. Chem.
767 Phys., 19(24), 15321–15337, doi:10.5194/acp-19-15321-2019, 2019.

https://doi.org/10.5194/acp-2020-1219
Preprint. Discussion started: 10 December 2020

Atmospheric Chemistry and Physics Discussions

768 Li, Q., Badia, A., Wang, T., Sarwar, G., Fu, X., Zhang, L., Zhang, Q., Fung, J., Cuevas, C.
769 A., Wang, S., Zhou, B. and Saiz-Lopez, A.: Potential Effect of Halogens on Atmospheric
770 Oxidation and Air Quality in China, J. Geophys. Res. Atmos., 1–21,
771 doi:10.1029/2019jd032058, 2020.

772 Liss, P. S. and Slater, P. G.: Flux of gases across air-sea interface, Nature, 247(5438), 181–
773 184, 1974.

774 MacDonald, S. M., Gómez Martín, J. C., Chance, R., Warriner, S., Saiz-Lopez, A.,
775 Carpenter, L. J. and Plane, J. M. C.: A laboratory characterisation of inorganic iodine
776 emissions from the sea surface: dependence on oceanic variables and parameterisation for
777 global modelling, Atmos. Chem. Phys., 14(11), 5841–5852, doi:10.5194/acp-14-5841-2014,
778 2014.

779 Mahajan, A. S., Oetjen, H., Saiz-Lopez, A., Lee, J. D., McFiggans, G. B. and Plane, J. M. C.:
780 Reactive iodine species in a semi-polluted environment, Geophys. Res. Lett., 36(L16803)
781 [online] Available from: http://dx.doi.org/10.1029/2009GL038018, 2009.

782 Mahajan, A. S., Shaw, M., Oetjen, H., Hornsby, K. E., Carpenter, L. J., Kaleschke, L., Tian-
783 Kunze, X., Lee, J. D., Moller, S. J., Edwards, P. M., Commane, R., Ingham, T., Heard, D. E.
784 and Plane, J. M. C.: Evidence of reactive iodine chemistry in the Arctic boundary layer, J.
785 Geophys. Res., 115(D20303,), doi:dx.doi.org/10.1029/2009JD013665, 2010a.

786 Mahajan, A. S., Plane, J. M. C., Oetjen, H., Mendes, L. M., Saunders, R. W., Saiz-Lopez, A.,
787 Jones, C. E., Carpenter, L. J. and McFiggans, G. B.: Measurement and modelling of
788 tropospheric reactive halogen species over the tropical Atlantic Ocean, Atmos. Chem. Phys.,
789 10, 4611–4624 [online] Available from: http://www.atmos-chem-phys.net/10/4611/2010/,
790 2010b.

791 Mahajan, A. S., Sorribas, M., Gómez Martín, J. C., MacDonald, S. M., Gil, M., Plane, J. M.

https://doi.org/10.5194/acp-2020-1219
Preprint. Discussion started: 10 December 2020

792 C. and Saiz-Lopez, A.: Concurrent observations of atomic iodine, molecular iodine and
793 ultrafine particles in a coastal environment, Atmos. Chem. Phys., 11, 2545–2555,
794 doi:10.5194/acpd-10-27227-2010, 2011.

795 Mahajan, A. S., Gómez Martín, J. C., Hay, T. D., Royer, S.-J., Yvon-Lewis, S. A., Liu, Y.,
796 Hu, L., Prados-Román, C., Ordóñez, C., Plane, J. M. C. and Saiz-Lopez, A.: Latitudinal
797 distribution of reactive iodine in the Eastern Pacific and its link to open ocean sources,
798 Atmos. Chem. Phys., 12, 11609–11617, doi:10.5194/acp-12-11609-2012, 2012.

799 Mahajan, A. S., Tinel, L., Hulswar, S., Cuevas, C. A., Wang, S., Ghude, S., Naik, R. K.,
800 Mishra, R. K., Sabu, P., Sarkar, A., Anilkumar, N. and Saiz Lopez, A.: Observations of
801 iodine oxide in the Indian Ocean marine boundary layer: A transect from the tropics to the
802 high latitudes, Atmos. Environ. X, 1, 100016, doi:10.1016/j.aeaoa.2019.100016, 2019a.

803 Mahajan, A. S., Tinel, L., Sarkar, A., Chance, R., Carpenter, L. J., Hulswar, S., Mali, P.,
804 Prakash, S. and Vinayachandran, P. N.: Understanding Iodine Chemistry over the Northern
805 and Equatorial Indian Ocean, J. Geophys. Res. Atmos., (x), 0–3,
806 doi:10.1029/2018JD029063, 2019b.

807 McFiggans, G. B.: Marine aerosols and iodine emissions, Nature, 433(7026), E13–E13, 2005.

808 Muñiz-Unamunzaga, M., Borge, R., Sarwar, G., Gantt, B., de la Paz, D., Cuevas, C. A. and
809 Saiz-Lopez, A.: The influence of ocean halogen and sulfur emissions in the air quality of a
810 coastal megacity: The case of Los Angeles, Sci. Total Environ., 610–611, 1536–1545,
811 doi:https://doi.org/10.1016/j.scitotenv.2017.06.098, 2018.

812 O'Dowd, C. D., Jimenez, J. L., Bahreini, R., Flagan, R. C., Seinfeld, J. H., Hämeri, K.,
813 Pirjola, L., Kulmala, M., Gerard Jennings, S., Hoffmann, T., Hameri, K. and Jennings, S. G.:
814 Marine aerosol formation from biogenic iodine emissions, Nature, 417(6889), 632–636,
815 doi:10.1038/nature00773.1.2.3.4.5.6.7.8.9.10., 2002.

https://doi.org/10.5194/acp-2020-1219
Preprint. Discussion started: 10 December 2020

816 O'Dowd, C. D., Facchini, M. C., Cavalli, F., Ceburnis, D., Mircea, M., Decesari, S., Fuzzi,
817 S., Yoon, Y. J., Putaud, J. P. and Dowd, C. D. O.: Biogenically driven organic contribution to
818 marine aerosol, Nature, 431(7009), 676–680, doi:10.1038/nature02970.1., 2004.

819 Platt, U. and Honninger, G.: The role of halogen species in the troposphere, Chemosphere,
820 52(2), 325–338, 2003.

821 Platt, U. and Janssen, C.: Observation and Role of the Free Radicals NO3 C10, BrO and I0 in
822 the Troposphere, Faraday Discuss., 1995.

823 Prados-Roman, C., Cuevas, C. a., Hay, T., Fernandez, R. P., Mahajan, A. S., Royer, S.-J.,
824 Galí, M., Simó, R., Dachs, J., Großmann, K., Kinnison, D. E., Lamarque, J.-F. and Saiz-
825 Lopez, A.: Iodine oxide in the global marine boundary layer, Atmos. Chem. Phys., 15(2),
826 583–593, doi:10.5194/acp-15-583-2015, 2015.

827 Qasim, S. Z.: Oceanography of the northern Arabian Sea, Deep Sea Res. Part A. Oceanogr.
828 Res. Pap., 29(9), 1041–1068, doi:https://doi.org/10.1016/0198-0149(82)90027-9, 1982.

829 Read, K. A., Mahajan, A. S., Carpenter, L. J., Evans, M. J., Faria, B. V. E., Heard, D. E.,
830 Hopkins, J. R., Lee, J. D., Moller, S. J., Lewis, A. C., Mendes, L. M., McQuaid, J. B., Oetjen,
831 H., Saiz-Lopez, A., Pilling, M. J. and Plane, J. M. C.: Extensive halogen-mediated ozone
832 destruction over the tropical Atlantic Ocean, Nature, 453(7199), 1232–1235,
833 doi:10.1038/nature07035, 2008.

834 Sahu, L. K., Lal, S. and Venkataramani, S.: Distributions of O3, CO and hydrocarbons over
835 the Bay of Bengal: A study to assess the role of transport from southern India and marine
836 regions during September-October 2002, Atmos. Environ., 40(24), 4633–4645,
837 doi:10.1016/j.atmosenv.2006.02.037, 2006.

838 Saiz-Lopez, A. and von Glasow, R.: Reactive halogen chemistry in the troposphere., Chem.

https://doi.org/10.5194/acp-2020-1219
Preprint. Discussion started: 10 December 2020

839 Soc. Rev., doi:10.1039/c2cs35208g, 2012.

840 Saiz-Lopez, A. and Plane, J. M. C.: Novel iodine chemistry in the marine boundary layer,
841 Geophys. Res. Lett., 31(4), L04112, doi:10.1029/2003GL019215, 2004.

842 Saiz-Lopez, A., Mahajan, A. S., Salmon, R. A., Bauguitte, S. J.-B., Jones, A. E., Roscoe, H.
843 K. and Plane, J. M. C.: Boundary Layer Halogens in Coastal Antarctica, Science (80-.).,
844 317(5836), 348–351, doi:10.1126/science.1141408, 2007.

845 Saiz-Lopez, A., Plane, J. M. C., Baker, A. R., Carpenter, L. J., von Glasow, R., Martín, J. C.
846 G., McFiggans, G. B., Saunders, R. W. and Gómez Martín, J. C.: Atmospheric Chemistry of
847 Iodine, Chem. Rev., 112(3), 1773–1804, doi:10.1021/cr200029u, 2012a.

848 Saiz-Lopez, A., Lamarque, J.-F., Kinnison, D. E., Tilmes, S., Ordóñez, C., Orlando, J. J.,
849 Conley, A. J., Plane, J. M. C., Mahajan, A. S., Sousa Santos, G., Atlas, E. L., Blake, D. R.,
850 Sander, S. P., Schauffler, S., Thompson, a. M. and Brasseur, G.: Estimating the climate
851 significance of halogen-driven ozone loss in the tropical marine troposphere, Atmos. Chem.
852 Phys., 12, 3939–3949, doi:10.5194/acp-12-3939-2012, 2012b.

853 Saiz-Lopez, A., Fernandez, R. P., Ordóñez, C., Kinnison, D. E., Gómez Martín, J. C.,
854 Lamarque, J.-F. and Tilmes, S.: Iodine chemistry in the troposphere and its effect on ozone,
855 Atmos. Chem. Phys., 14(23), 13119–13143, doi:10.5194/acp-14-13119-2014, 2014.

856 Saiz-Lopez, A., Plane, J. M. C., Cuevas, C. A., Mahajan, A. S., Lamarque, J.-F. and
857 Kinnison, D. E.: Nighttime atmospheric chemistry of iodine, Atmos. Chem. Phys., 16(24),
858 15593–15604, doi:10.5194/acp-16-15593-2016, 2016.

859 Sarwar, G., Gantt, B., Schwede, D., Foley, K., Mathur, R. and Saiz-Lopez, A.: Impact of
860 Enhanced Ozone Deposition and Halogen Chemistry on Tropospheric Ozone over the
861 Northern Hemisphere, Environ. Sci. Technol., 49(15), 9203–9211,

https://doi.org/10.5194/acp-2020-1219
Preprint. Discussion started: 10 December 2020

862 doi:10.1021/acs.est.5b01657, 2015.

863 Seitz, K., Buxmann, J., Pöhler, D., Sommer, T., Tschritter, J., Neary, T., O'Dowd, C. D. and
864 Platt, U.: The spatial distribution of the reactive iodine species IO from simultaneous active
865 and passive DOAS observations, Atmos. Chem. Phys., 10(5), 2117–2128 [online] Available
866 from: http://www.atmos-chem-phys.net/10/2117/2010/, 2010.

867 Sellegri, K., Pey, J., Rose, C., Culot, A., DeWitt, H. L., Mas, S., Schwier, A. N., Temime-
868 Roussel, B., Charriere, B., Saiz-Lopez, A., Mahajan, A. S., Parin, D., Kukui, A., Sempere, R.,
869 D'Anna, B. and Marchand, N.: Evidence of atmospheric nanoparticle formation from
870 emissions of marine microorganisms, Geophys. Res. Lett., 43(12), 6596–6603,
871 doi:10.1002/2016GL069389, 2016.

872 Sherwen, T., Evans, M. J. J., Carpenter, L. J. J., Andrews, S. J. J., Lidster, R. T. T., Dix, B.,
873 Koenig, T. K. K., Volkamer, R., Saiz-Lopez, A., Prados-Roman, C., Mahajan, A. S.,
874 Ordóñez, C., Sinreich, R. and Ortega, I.: Iodine's impact on tropospheric oxidants: a global
875 model study in GEOS-Chem, Atmos. Chem. Phys., 16(2), 1161–1186, doi:10.5194/acp-16-
876 1161-2016, 2016.

877 Simpson, W. R., Brown, S. S., Saiz-Lopez, A., Thornton, J. a. and Glasow, R. Von:
878 Tropospheric Halogen Chemistry: Sources, Cycling, and Impacts, Chem. Rev.,
879 150312153236002, doi:10.1021/cr5006638, 2015.

880 Sommariva, R., Bloss, W. J. and von Glasow, R.: Uncertainties in gas-phase atmospheric
881 iodine chemistry, Atmos. Environ., 57, 219–232, doi:10.1016/j.atmosenv.2012.04.032, 2012.

882 Stone, D., Sherwen, T., Evans, M. J., Vaughan, S., Ingham, T., Whalley, L. K., Edwards, P.
883 M., Read, K. A., Lee, J. D., Moller, S. J., Carpenter, L. J., Lewis, A. C. and Heard, D. E.:
884 Impacts of bromine and iodine chemistry on tropospheric OH and HO2: Comparing
885 observations with box and global model perspectives, Atmos. Chem. Phys., doi:10.5194/acp-

https://doi.org/10.5194/acp-2020-1219
Preprint. Discussion started: 10 December 2020

886 18-3541-2018, 2018.

887 Stutz, J., Pikelnaya, O., Hurlock, S. C., Trick, S., Pechtl, S. and von Glasow, R.: Daytime
888 OIO in the gulf of Maine, Geophys. Res. Lett., 34(22), L22816, 2007.

889 Travis, K. R., Heald, C. L., Allen, H. M., Apel, E. C., Arnold, S. R., Blake, D. R., Brune, W.
890 H., Chen, X., Commane, R., Crounse, J. D., Daube, B. C., Diskin, G. S., Elkins, J. W., Evans,
891 M. J., Hall, S. R., Hintsa, E. J., Hornbrook, R. S., Kasibhatla, P. S., Kim, M. J., Luo, G.,
892 McKain, K., Millet, D. B., Moore, F. L., Peischl, J., Ryerson, T. B., Sherwen, T., Thames, A.
893 B., Ullmann, K., Wang, X., Wennberg, P. O., Wolfe, G. M. and Yu, F.: Constraining remote
894 oxidation capacity with ATom observations, Atmos. Chem. Phys., 20(13), 7753–7781,
895 doi:10.5194/acp-20-7753-2020, 2020.

896 Wada, R., Beames, J. M. and Orr-Ewing, A. J.: Measurement of IO radical concentrations in
897 the marine boundary layer using a cavity ring-down spectrometer, J. Atmos. Chem., 58, 69–
898 87, 2007.

899 Wang, F., Saiz-Lopez, A., Mahajan, A. S., Gómez Martín, J. C., Armstrong, D., Lemes, M.,
900 Hay, T. and Prados-Roman, C.: Enhanced production of oxidised mercury over the tropical
901 Pacific Ocean: a key missing oxidation pathway, Atmos. Chem. Phys., 14(3), 1323–1335,
902 doi:10.5194/acp-14-1323-2014, 2014.

903 Wayne, R. P., Barnes, I., Biggs, P., Burrows, J. P., Canosamas, C. E., Hjorth, J., Lebras, G.,
904 Moortgat, G. K., Perner, D., Poulet, G., Restelli, G. and Sidebottom, H.: The Nitrate Radical -
905 Physics, Chemistry, and the Atmosphere, Atmos. Environ. Part a-General Top., 25(1), 1–203,
906 1991.

907 Zingler, J. and Platt, U.: Iodine oxide in the Dead Sea Valley: Evidence for inorganic sources
908 of boundary layer IO, J. Geophys. Res. - Atmos., 110(D7), D07307, 2005.

https://doi.org/10.5194/acp-2020-1219
Preprint. Discussion started: 10 December 2020

Atmospheric Chemistry and Physics Discussions

909 Ziska, F., Quack, B., Abrahamsson, K., Archer, S. D., Atlas, E. L., Bell, T., Butler, J. H.,
910 Carpenter, L. J., Jones, C. E., Harris, N. R. P., Hepach, H., Heumann, K. G., Hughes, C.,
911 Kuss, J., Krüger, K., Liss, P., Moore, R. M., Orlikowska, a., Raimund, S., Reeves, C. E.,
912 Reifenhäuser, W., Robinson, a. D., Schall, C., Tanhua, T., Tegtmeier, S., Turner, S., Wang,
913 L., Wallace, D., Williams, J., Yamamoto, H., Yvon-Lewis, S. A. and Yokouchi, Y.: Global
914 sea-to-air flux climatology for bromoform, dibromomethane and methyl iodide, Atmos.
915 Chem. Phys., 13(17), 8915–8934, doi:10.5194/acp-13-8915-2013, 2013.

916

https://doi.org/10.5194/acp-2020-1219
Preprint. Discussion started: 10 December 2020

Atmospheric Chemistry and Physics Discussions

Tables

Table 1: Monthly mean of IO concentration in parts per trillion by volume (pptv) over the domain region for model simulations in January, April, and July 2015, and simulation scenarios orgI, HAL and difference between HAL-orgI, before and after applying a land mask over the model domain.

IO (pptv)	Jan	April	July
Over the whole domain			
orgI	0.011±0.009	0.008±0.006	0.012±0.009
HAL	0.47±0.32	0.48±0.33	0.15±0.15
HAL-orgI	0.46±0.31	0.47±0.32	0.14±0.14
Only over the MBL			
orgI	0.015±0.009	0.011±0.006	0.015±0.008
HAL	0.63±0.20	0.64±0.22	0.19±0.14
HAL-orgI	0.62±0.20	0.63±0.21	0.18±0.14

https://doi.org/10.5194/acp-2020-1219
Preprint. Discussion started: 10 December 2020

Atmospheric Chemistry and Physics Discussions

924 **Table 2:** Monthly means and standard deviations of O_3, NO_2, NO, NO_3, OH, HO_2 mixing
925 ratios (unit in parenthesis) over the domain region for the model simulations in January,
926 April, and July for the HAL scenario along with the difference and percentage differences
927 between HAL and BASE. The table also includes monthly mean values only over the
928 MBL.

	January	April	July	January	April	July
	O_3 (ppbv)			**NO_3 (pptv)**		
	Over the whole domain					
HAL	32.16±9.76	29.64±10.79	23.34±8.85	7.64±8.08	10.38±15.53	4.52±6.14
HAL-BASE	-1.20±0.77	-0.97±0.71	0.01±0.31	-0.39±0.43	-0.33±0.83	-0.03±0.29
HAL-BASE %	-3.6±3.33	-3.16±3.62	0.06±1.37	-4.85±14.07	-3.09±10.72	-0.64±8.08
	Only over the MBL					
HAL	28.17±7.83	24.17±6.42	19.49±5.97	4.47±5.44	2.99±4.09	2.38±3.94
HAL-BASE	-1.31±0.67	-1.22±0.65	-0.10±0.21	-0.43±0.34	-0.27±0.31	-0.08±0.19
HAL-BASE %	-4.43±3.39	-4.80±3.49	-0.51±1.26	-8.80±14.41	-8.23±10.49	-3.14±8.29
	NO_2 (ppbv)			**OH (pptv)**		
	Over the whole domain					
HAL	0.43±1.27	0.30±0.77	0.27±0.79	0.14±0.05	0.26±0.07	0.28±0.08
HAL-BASE	-0.0040±0.0209	0.0007±0.0195	0.0003±0.0129	0.001±0.006	0.006±0.007	-0.003±0.006
HAL-BASE %	-0.91±11.08	0.22±6.89	0.10±5.85	0.34±4.54	2.55±2.47	-0.94±2.22
	Only over the MBL					
HAL	0.10±0.46	0.06±0.30	0.07±0.29	0.15±0.05	0.27±0.08	0.27±0.08
HAL-BASE	-0.0025±0.0071	-0.0005±0.0070	-0.0008±0.0061	0.001±0.007	0.007±0.007	-0.002±0.006
HAL-BASE %	-2.42±11.62	-0.91±7.19	-1.19±6.24	0.44±5.06	2.62±2.35	-0.67±2.23
	NO (pptv)			**HO_2 (pptv)**		
	Over the whole domain					
HAL	49.49±221.23	36.66±164.95	38.79±173.78	7.10±1.49	10.18±1.64	9.24±1.97
HAL-BASE	-0.23±5.83	0.59±6.49	-0.09±4.44	-0.48±0.43	-0.35±0.38	-0.19±0.16
HAL-BASE %	-0.47±15.32	1.64±10.85	-0.23±7.35	-6.39±5.54	-3.28±4.04	-2.03±1.71
	Only over the MBL					
HAL	12.56±85.76	10.38±77.48	11.64±58.45	7.32±1.12	9.80±1.36	8.67±1.53
HAL-BASE	-0.25±2.85	0.16±2.87	-0.20±1.99	-0.67±0.36	-0.53±0.26	-0.23±0.14
HAL-BASE %	-1.96±15.6	1.54±11.6	-1.71±7.73	-8.36±4.56	-5.14±3.05	-2.60±1.53

929

https://doi.org/10.5194/acp-2020-1219
Preprint. Discussion started: 10 December 2020

Atmospheric Chemistry and Physics Discussions

930 **Table 3:** Monthly means and standard deviations of O_3, NO_2, NO, NO_3, OH, HO_2 mixing
931 ratios (unit in parenthesis) over the domain region for the model simulations in January,
932 April, and July for the HAL scenario along with the absolute difference and absolute
933 difference percentage between HAL and BASE. The table also includes monthly mean
934 values only over the MBL.

	January	April	July	January	April	July
	O_3 (ppbv)			**NO_3 (pptv)**		
	Over the whole domain					
HAL	32.16±9.76	29.64±10.79	23.34±8.85	7.64±8.08	10.38±15.53	4.52±6.14
HAL-BASE	1.25±0.69	0.98±0.69	0.21±0.22	0.46±0.35	0.50±0.74	0.16±0.25
HAL-BASE %	3.75±3.17	3.21±3.58	0.89±1.04	5.73±13.6	4.68±9.78	3.52±6.84
	Only over the MBL					
HAL	28.17±7.83	24.17±6.42	19.49±5.97	4.47±5.44	2.99±4.09	2.38±3.94
HAL-BASE	1.31±0.66	1.22±0.65	0.15±0.18	0.45±0.31	0.29±0.29	0.11±0.17
HAL-BASE %	4.45±3.37	4.80±3.49	0.77±1.13	9.20±14.15	8.81±10.08	4.55±7.47
	NO_2 (ppbv)			**OH (pptv)**		
	Over the whole domain					
HAL	0.43±1.27	0.30±0.77	0.27±0.79	0.14±0.05	0.26±0.07	0.28±0.08
HAL-BASE	0.008±0.019	0.007±0.018	0.004±0.012	0.004±0.004	0.008±0.005	0.005±0.004
HAL-BASE %	1.89±10.63	2.15±5.71	1.63±5.33	3.29±3.14	3.02±1.94	1.82±1.40
	Only over the MBL					
HAL	0.10±0.46	0.06±0.30	0.07±0.29	0.15±0.05	0.27±0.08	0.27±0.08
HAL-BASE	0.004±0.007	0.002±0.007	0.002±0.006	0.005±0.004	0.008±0.005	0.005±0.004
HAL-BASE %	3.47±11.25	3.51±6.08	2.52±5.95	3.64±3.39	3.05±1.89	1.75±1.36
	NO (pptv)			**HO_2 (pptv)**		
	Over the whole domain					
HAL	49.49±221.23	36.66±164.95	38.79±173.78	7.10±1.49	10.18±1.64	9.24±1.97
HAL-BASE	1.60±5.61	1.57±6.33	1.03±4.32	0.51±0.39	0.44±0.27	0.21±0.14
HAL-BASE %	3.22±14.32	4.36±8.15	2.64±6.46	6.76±4.87	4.16±3.09	2.18±1.52
	Only over the MBL					
HAL	12.56±85.76	10.38±77.48	11.64±58.45	7.32±1.12	9.8±1.36	8.67±1.53
HAL-BASE	0.70±2.78	0.72±2.78	0.45±1.95	0.67±0.36	0.53±0.25	0.23±0.14
HAL-BASE %	5.48±14.86	7.07±8.58	3.76±7.15	8.38±4.51	5.17±2.98	2.63±1.49

935

https://doi.org/10.5194/acp-2020-1219
Preprint. Discussion started: 10 December 2020

Atmospheric Chemistry and Physics Discussions

936 **Figures**

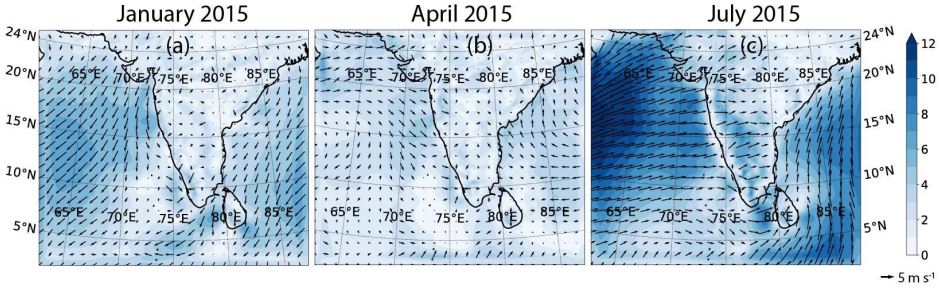

937

938 **Figure 1:** The wind direction and speed over the model domain during the three months used
939 to study the impact of iodine chemistry on the marine boundary layer. The three months
940 represent different seasons: the winter monsoon period in January, pre-monsoon in April and
941 the summer monsoon in July. The direction of the arrows shows the wind direction, and the
942 size of the arrows and the contour colours show the magnitude of the wind.

943

https://doi.org/10.5194/acp-2020-1219
Preprint. Discussion started: 10 December 2020

Atmospheric Chemistry and Physics Discussions

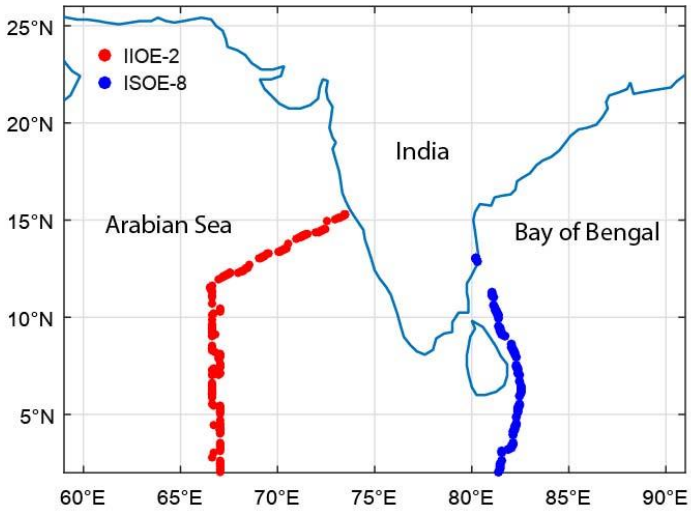

944

945 **Figure 2:** The domain chosen for the model runs along with the tracks of the cruises from
946 which data was used for validation are shown. The two cruises were the 2nd International Indian
947 Ocean Expedition (IIOE-2; December 2015) and the 8th Indian Southern Ocean Expedition
948 (ISOE-8; January 2015) and started from the West and East coast of India, respectively.

949

https://doi.org/10.5194/acp-2020-1219
Preprint. Discussion started: 10 December 2020

Atmospheric Chemistry and Physics Discussions

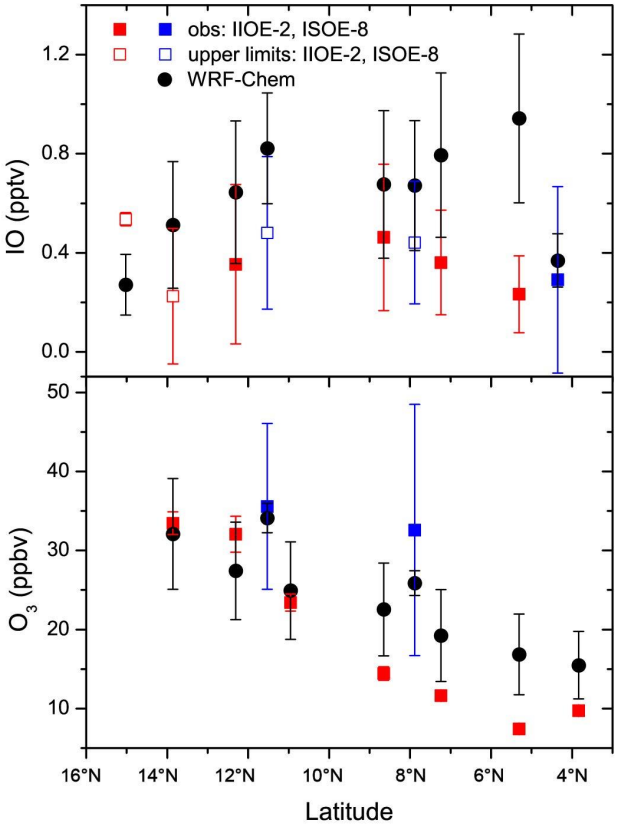

950

951 **Figure 3:** A comparison between the model simulated and observed IO (top panel) and O_3
952 (bottom panel) is shown. In cases where IO was not detected, an upper limit (empty squares)
953 was estimated.

954

https://doi.org/10.5194/acp-2020-1219
Preprint. Discussion started: 10 December 2020

Atmospheric Chemistry and Physics Discussions

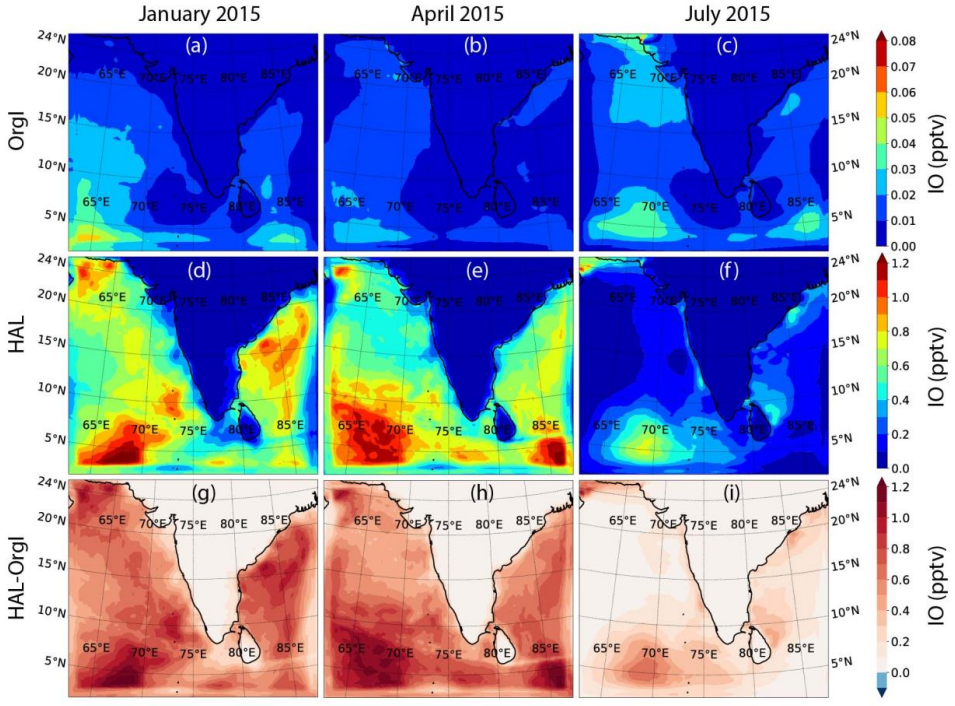

955

956 **Figure 4:** Model simulation showing the boundary layer averaged IO mixing ratios across the
957 domain during the three seasons, along with a difference between the HAL and orgI scenarios
958 for each season are shown.

959

https://doi.org/10.5194/acp-2020-1219
Preprint. Discussion started: 10 December 2020

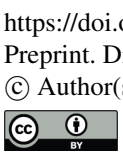

Atmospheric Chemistry and Physics Discussions

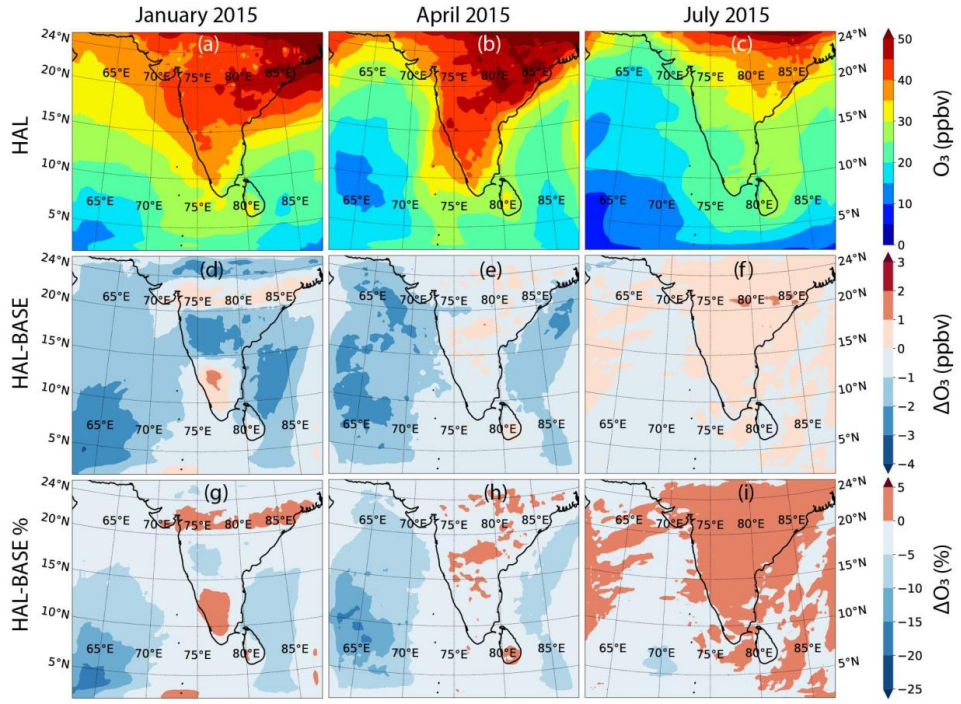

960

961 **Figure 5:** Model simulations showing the boundary layer averaged O_3 mixing ratios across the
962 domain during the three seasons for the HAL scenario (top panels), along with the differences
963 (middle panels) and the percentage differences (lower panels) between the HAL and BASE
964 scenarios for each season are shown.

965

https://doi.org/10.5194/acp-2020-1219
Preprint. Discussion started: 10 December 2020

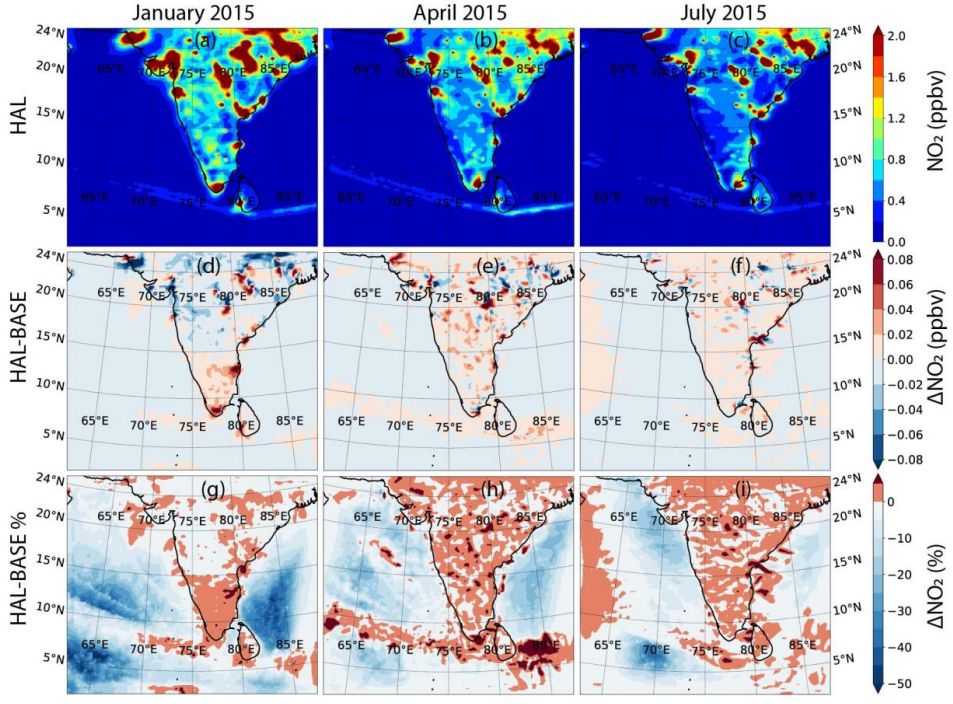

966

967 **Figure 6:** Model simulations showing the boundary layer averaged NO_2 mixing ratios across
968 the domain during the three seasons for the HAL scenario (top panels), along with the
969 differences (middle panels) and the percentage differences (lower panels) between the HAL
970 and BASE scenarios for each season are shown.

971

https://doi.org/10.5194/acp-2020-1219
Preprint. Discussion started: 10 December 2020

Atmospheric Chemistry and Physics Discussions

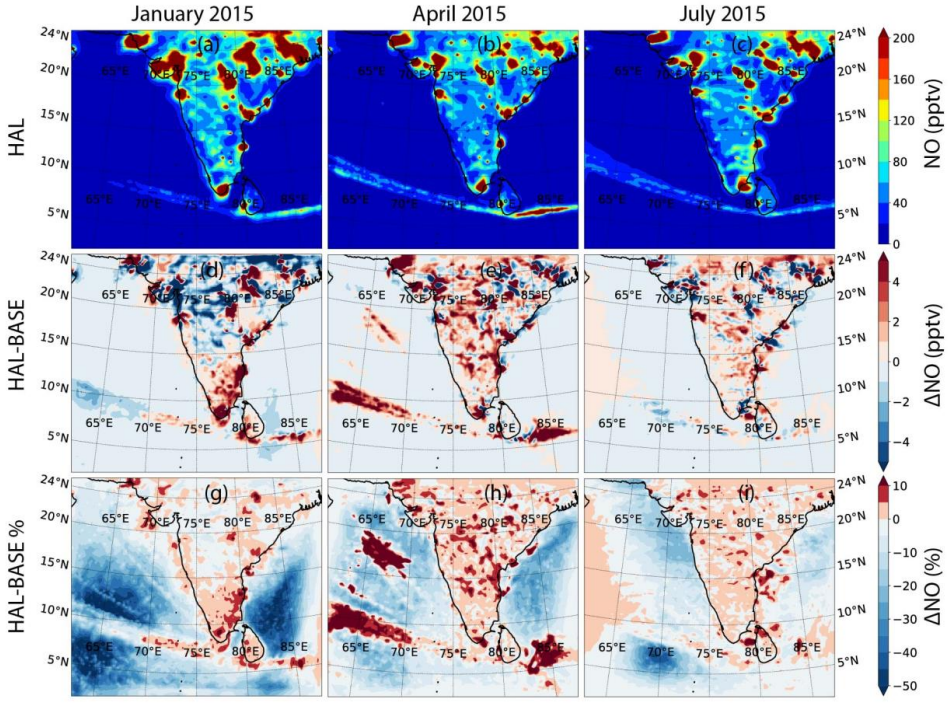

Figure 7: Model simulations showing the boundary layer averaged NO mixing ratios across the domain during the three seasons for the HAL scenario (top panels), along with the differences (middle panels) and the percentage differences (lower panels) between the HAL and BASE scenarios for each season are shown.

https://doi.org/10.5194/acp-2020-1219
Preprint. Discussion started: 10 December 2020

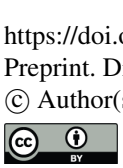

Atmospheric Chemistry and Physics Discussions

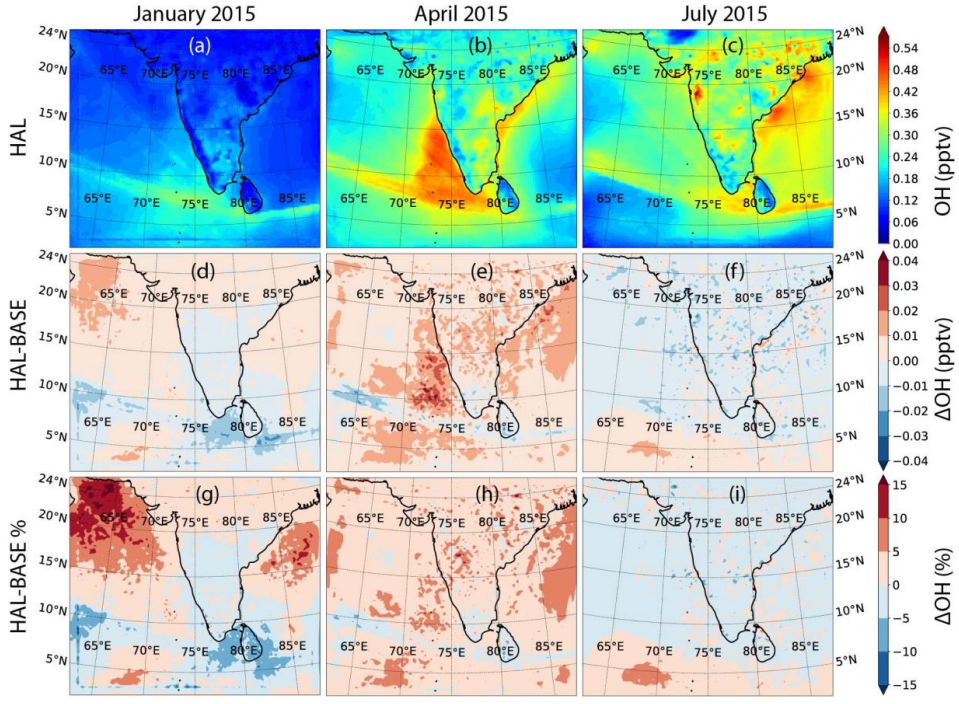

978

979 **Figure 8:** Model simulations showing the boundary layer averaged OH mixing ratios across
980 the domain during the three seasons for the HAL scenario (top panels), along with the
981 differences (middle panels) and the percentage differences (lower panels) between the HAL
982 and BASE scenarios for each season are shown.

983

https://doi.org/10.5194/acp-2020-1219
Preprint. Discussion started: 10 December 2020

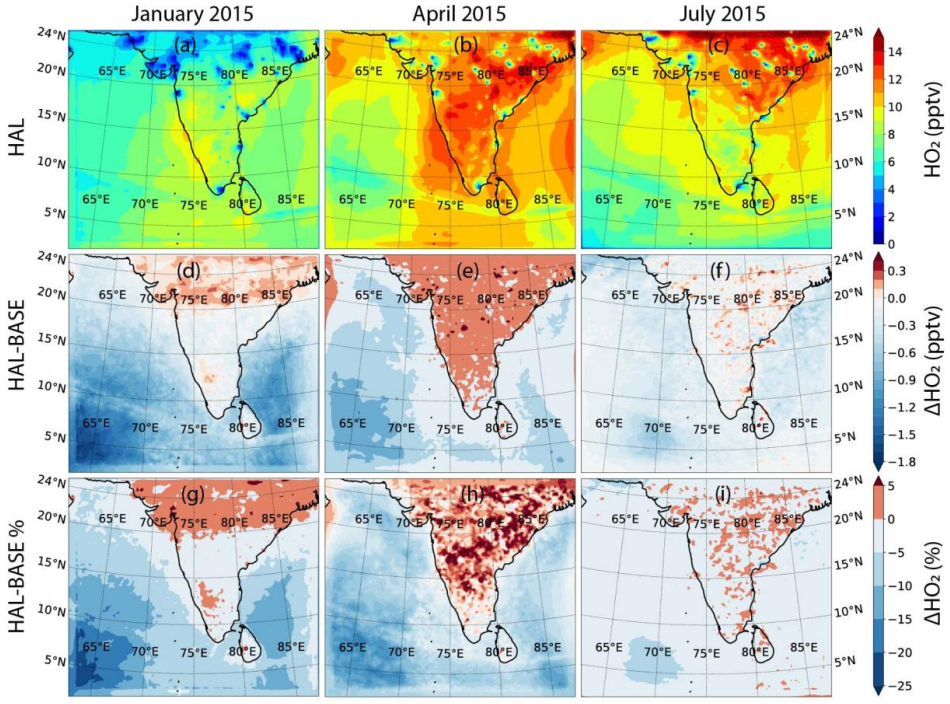

Figure 9: Model simulations showing the boundary layer averaged HO_2 mixing ratios across the domain during the three seasons for the HAL scenario (top panels), along with the differences (middle panels) and the percentage differences (lower panels) between the HAL and BASE scenarios for each season are shown.

https://doi.org/10.5194/acp-2020-1219
Preprint. Discussion started: 10 December 2020

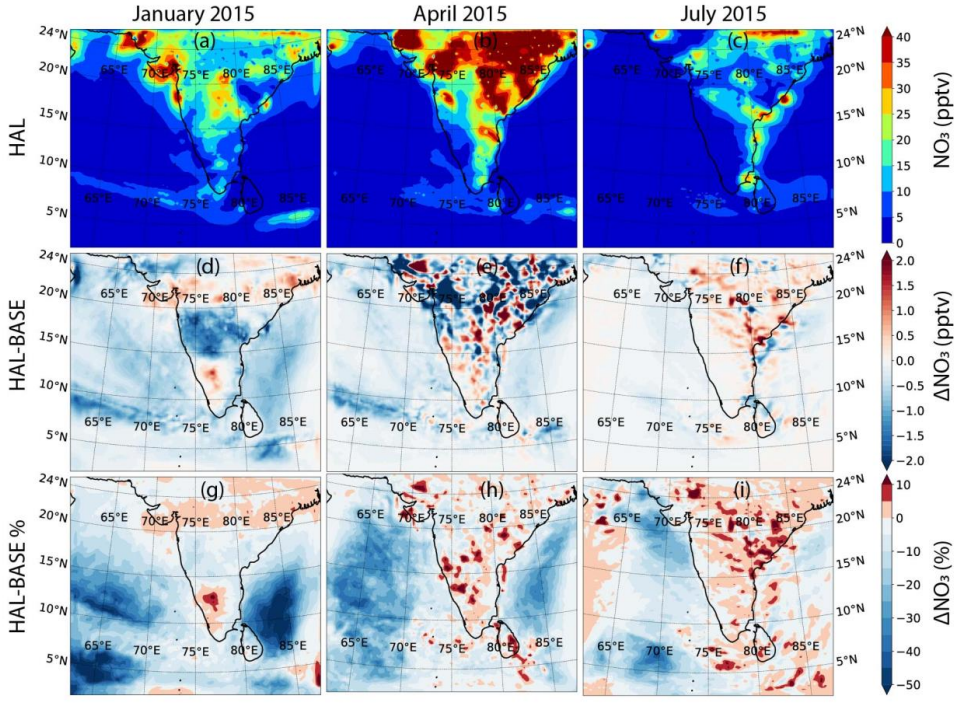

Figure 10: Model simulations showing the boundary layer averaged NO_3 mixing ratios across the domain during the three seasons for the HAL scenario (top panels), along with the differences (middle panels) and the percentage differences (lower panels) between the HAL and BASE scenarios for each season are shown.